Urban Water Journal

ISSN: (Print) (Online) Journal homepage: https://www.tandfonline.com/loi/nurw20

How much green roofs and rainwater harvesting systems can contribute to urban flood mitigation?

Elena Cristiano, Stefano Farris, Roberto Deidda & Francesco Viola

To cite this article: Elena Cristiano, Stefano Farris, Roberto Deidda & Francesco Viola (2022): How much green roofs and rainwater harvesting systems can contribute to urban flood mitigation?, Urban Water Journal, DOI: 10.1080/1573062X.2022.2155849

To link to this article: https://doi.org/10.1080/1573062X.2022.2155849

Published online: 27 Dec 2022.

URBAN WATER JOURNAL
https://doi.org/10.1080/1573062X.2022.2155849

Taylor & Francis
Taylor & Francis Group

RESEARCH ARTICLE

OPEN ACCESS Check for updates

How much green roofs and rainwater harvesting systems can contribute to urban flood mitigation?

Elena Cristiano, Stefano Farris, Roberto Deidda and Francesco Viola

Dipartimento di Ingegneria Civile, Ambientale e Architettura, Università degli Studi di Cagliari, Cagliari, Italy

ABSTRACT

Increased urbanization combined with the intensification of short rainfall events has worsened the urban flood issue. Among the different blue-green solutions to mitigate pluvial floods, green roofs (GR) and rainwater harvesting (RWH) have been investigated as sustainable systems to reduce runoff from rooftops. Their flood mitigation capacity, however, has been estimated mostly at building-scale. Following the need to estimate discharge reduction at large scale over entire cities, we simulated the installation of (extensive, intensive and multilayer blue) GRs on flat roofs and RWH systems for sloped ones. Performances of such systems were investigated in selected cities, representing different climate regimes. Although at building-scale GRs showed higher retention capacity, the cost-efficiency analysis highlights that at large-scale RWH tanks ensure higher retention with lower costs, due to rooftop distribution. The coupled system of multilayer blue-GRs and RWH tanks guarantees a discharge reduction of 5% even during extreme events.

ARTICLE HISTORY
Received 24 February 2022
Accepted 1 December 2022

KEYWORDS
Green roof; multilayer blue-green roof; pluvial flood mitigation; rainwater harvesting; urban scale; sustainable development

1. Introduction

The number of people living in cities is growing fast and by 2050 it is expected that 68% of the total population will have moved to urban areas (UN 2018), with a consequent increase of urban density and impervious surfaces (Duncan Black and Vernon Henderson 1999; Anon 2016; Rademacher 2019). At the same time, climate change is likely to lead to an intensification of rainfall extremes (Myhre et al. 2019; Liu et al. 2019b; IPCC 2022). Fast urban growth coupled with climate changes is likely to trigger the increase of pluvial flood risk in many regions. Several studies proposed different solutions to mitigate flood risk (Sahani et al. 2019; Liu, Fryd, and Zhang 2019a; Depietri and McPhearson 2017), focusing on reducing and delaying the runoff generation from rooftops (Fletcher et al. 2015; LÖwe et al. 2017). Green roofs (GRs) and rainwater harvesting (RWH) systems have shown to be among the most flexible, sustainable and efficient solutions to mitigate the urban runoff generation (Mentens, Raes, And Hermy 2006; Depietri and McPhearson 2017). These tools have been largely investigated at building scale, evaluating the runoff generation reduction that can be achieved from a single GR or RWH system installation. Only a few studies have analysed the potential benefits of the installation of either GRs or RWH systems at urban scale (i.e. analysing the effects of the installation of these solutions on multiple buildings of an entire city) and no study has considered the installation of both tools in the same area. The most relevant works available in literature are examined as follows: firstly, studies concerning the GR and RWH mitigation capacity at single building scale are illustrated, and secondly references that discuss the potential impacts of these solutions at urban scale are summarized.

GRs allow water to be captured in a sustainable way (Rosasco and Perini 2019): during the storm event, a portion of rainfall is retained in the soil layer and later absorbed by the vegetation roots and used to feed evapotranspiration dynamics (Locatelli et al. 2014; Stovin, Vesuviano, and Kasmin 2012; Vijayaraghavan 2016; Liu et al. 2020; Schultz, Sailor, and Starry 2018). Beside their capacity to retain water, GRs also exert an action of detaining rain, delaying, and mitigating the flood generation. Retention performances of GRs depend on soil thickness and type, and vegetation species. A thinner soil layer, on one hand, is flexible to manage and easy to install, but does not ensure a large retention performance, with a consequent small contribution to the discharge reduction. Besides flood mitigation, GRs have shown multiple benefits for the urban environment, guaranteeing the growth of urban ecosystems and thus enhancing biodiversity (Oberndorfer et al. 2007; Wooster et al. 2022; Gonsalves et al. 2022). Moreover, GRs contribute to reducing the heat island effect, lowering the surrounding temperature (Solcerova et al. 2017; Khare, Vajpai, and Gupta 2021; Dwivedi and Mohan 2018) and ensuring thermal insulation for the building (Bevilacqua 2021; He et al. 2020). These solutions can help reduce water pollution, since the soil layer can retain several contaminants, and, at the same time, GRs increase the aesthetic value of the city (Berardi, Ghaffarianhoseini, and Ghaffarianhoseini 2014; Cipolla et al. 2018).

RWH systems were developed in Mediterranean areas in ancient times, with the aim of collecting rainfall from rooftops, storing it in tanks, and reusing it for irrigation during dry periods (Beckers, Berking, and Schütt 2013; Velasco-Muñoz et al. 2019). Since then, RWH systems have been largely developed and applied in urban areas for both private and public buildings, where the collected rainwater can be used for domestic non-

CONTACT Elena Cristiano elena.cristiano@unica.it

potable purposes, such as garden irrigation or toilet flushing (Adugna et al. 2018; Akter and Ahmed 2015; Campisano et al. 2017; Teston et al. 2022). RWH systems, hence, can reduce the pressure on the supply systems, especially in areas characterized by long hot and dry periods (Molaei, Kouchakzadeh, and Fashi 2019; Palla, Gnecco, and Barbera 2017). In addition, the collected rainwater can be used to recharge the groundwater (Nachson et al. 2022; Rajasekhar et al. 2020). Moreover, in urban areas, the installation of RWH systems can mitigate pluvial floods, since a large volume of rainfall is retained in the water tanks and does not contribute to the runoff generation (Huang et al. 2015; Freni and Liuzzo 2019; Araujo et al. 2021; Jamali, Bach, and Deletic 2020). Consequently, the outflow peak is reduced, contributing to a better management of the urban drainage system (Palla, Gnecco, and Barbera 2017). While RWH systems have shown good performance in different climate conditions (Palla et al. 2012) and their installation is straight forward, their drawback is that water tanks require large volumes, that might not be available, especially in old cities with narrow streets, and can be anti-aesthetic.

An innovative nature-based solution, that combines the multiple GR benefits with the large water storage capacity typical of RWH systems, is the multilayer blue-green roof (MBGR) (Andenæs et al. 2018; Pelorosso et al. 2021; Cristiano, Deidda, and Viola 2021a). Compared to traditional GRs, MBGRs present an additional layer, that enables the water that percolates from the soil to be collected and stored for a potential reuse. Since it combines the retention capacity of a traditional GR and the detention capacity of a RWH tank, the achievable MBGRs runoff generation reduction is quite high (Busker et al. 2022; Martin and Kaye 2020), and at the same time, MBGRs show all the benefits that characterize the traditional GR (e.g. building thermal insulation, urban heat island reduction, biodiversity increase, etc.). Following an integrated Water-Energy-Food-Ecosystem (WEFE) Nexus approach, where benefits and limitation are investigated analysing the impact on multiple fields at the same time, MBGRs show high potential in the achievement of the United Nation Sustainable Development Goals of the 2030 Agenda (SDGs) (Cristiano, Deidda, and Viola 2021a; Calheiros and Stefanakis 2021; Gomes et al. 2021; Wright et al. 2021).

At urban scale, Karteris et al. (2016) analysed the potential benefits of GR installation on flat roofs in Thessaloniki, a large Greek city. Results showed a mean GR retention performance of 45% of the total rainfall, that can reach 71% for some buildings. A similar study, proposed by Zhou et al. (2019), investigated the flood mitigation performance of GR at large scale, in a neighbourhood of Beijing (China). Buildings were selected through a supervised classification and a manual identification of the non-suitable buildings, such as cultural relics and historic sites. Their study highlights that effective runoff reduction can be achieved by installing GRs in 50% of the suitable sites.

The potential impact of installing rainwater harvesting systems at large scale on stormwater retention was evaluated by Freni and Liuzzo (2019). They analysed the benefits of installing 208 tanks of 5 m^3 in a 1.6 km^2 residential area of Sicily (Southern Italy) through a model simulation. The flooded area was reduced by up to 35% for rainfall events with a depth of up to 50 mm, while for severe rainfall events the reduction was negligible.

While the potential benefits of large-scale GR installation have been investigated by Karteris et al. (2016) and Zhou et al. (2018) on one hand, and those related to large-scale RWH installation by Freni and Liuzzo (2019) on the other hand, there is still a lack of studies of GR and RWH mixed solutions, including the installation of MBGRs and climatic conditions. The impacts of large-scale GR, MBGR and RWH implementation, even considering mixed solutions, in terms of flood reduction efficiency and economic costs needs further investigations. Given all the above premises on GRs, MBGRs and RWH systems, the aim of this work is to investigate the potential impact of installing these solutions in large cities, explicitly accounting for local climates and urban features. The influence of climate in determining the impact of GRs, MBGRs and RWH infrastructures has been considered by selecting nine representative cities around the globe, while urban features analysis have been here epitomized by roof slope and area distribution at each location derived from freely available Digital Surface Models (DSM). Different techniques and approaches have been proposed in literature to identify specific features of buildings, or groups of buildings. Building recognition from satellite images is a common approach in urban planning, with the goal to monitor and predict possible developments (Chen, Gao, and Devereux 2017). The analysis of roof distribution and geometrical roof properties can provide useful information not only for the installation of pluvial flood mitigation solutions, but also for all the studies that involve a large urban scale application, e.g. photovoltaic panel installation (Mainzer et al. 2017) and urban turbulence (Garau et al. 2018). The DSM, obtained from Lidar images, has been largely used to identify buildings (Wen et al. 2019) or vegetation and green areas (Ellis and Mathews 2019) through different techniques. Some recent studies proposed automatic roof detection algorithms based on in-depth learning and neural network techniques (Zhang, Zhang, and Du 2016; Alidoost and Arefi 2018). These approaches provide a good identification of roofs and vegetation, but they are computationally demanding in terms of CPU time and power. In our study, we implemented an alternative approach, which is commonly used to identify roofs by comparing DSM and Digital Terrain Model (DTM), which represents the elevation of the terrain, without buildings and vegetation (Li, Lin, and Shimamura 2008; Yu et al. 2010). The difference between the 2 layers allows all the objects on the surface to be detected. This method, however, is limited by the fact that both DSM and DTM should be available at high resolution for the investigated area (Beumier and Idrissa 2016; Weidner 1997).

The current work presents a twofold extension starting from such preliminary results discussed in Cristiano et al. (2021b) on the potential impacts of a large-scale installation of GR and RWH systems, considering also the potential implementation of MBGR at large scale and introducing a different approach, which enables both building-scale and large-scale impact of blue-green solutions to be investigated. Results are illustrated here considering their distribution and variability: in particular, the time between rainfall and runoff generation is analysed here following a probabilistic approach, which enables the results to be better understood and supported.

The paper is structured as follows. In Section 2 case studies and available climatological data are described. Section 3 explains the approach developed to analyse runoff mitigation effects achievable with the installation of GRs, MBGRs and/or RWH systems for different scenarios and conditions, focusing on the roof slope identification and discharge estimation. Results are illustrated and discussed in Section 4, where a cost-efficiency analysis has also been conducted in order to estimate the potential cost of a large-scale installation of the different solutions and to identify the most suitable option. Section 5 summarises the work presented and the main conclusions.

2. Case studies

2.1. Site description

Nine cities with a different climatological characterization and geographical location have been selected as case studies. Cities were chosen worldwide in order to elect at least one representative of four different climatic conditions, as described in Viola, Hellies, and Deidda (2017); this classification was made by comparing the phase between monthly mean rainfall and potential evapotranspiration (ETP) seasonal cycles. The first climate case (A) is characterized by constant rainfall throughout the year and one seasonal ETP peak: these elements are typical of the North European and American climate, which present higher potential evapotranspiration in summer than in winter; London (UK), Waterloo (Canada) and Montreal (Canada) were selected as representative of climate case A. Constant ETP and one seasonal rainfall peak define the second climate case (B): this scenario characterizes the equatorial area; a small urban area in Haiti belongs to this case. Continental climates are represented in the third climate case (C) when ETP and rainfall are in phase: for this scenario, the town of Airdrie (Canada) was selected. Asynchronous peaks of ETP and rainfall describe the last climate scenario (D): intense rainfall events during the cold season alternated with long dry and hot periods are typical of coastal and Mediterranean areas; to represent this climate, we choose Cagliari (Italy), Auckland (New Zealand), Wellington (New Zealand) and Vancouver (Canada).

For the selected cities, the DSM at 1 m resolution and a vector layer with building footprints were freely available (see Table 1's footnotes for the data links). In the case of London, the DSM was evaluated at 2 m resolution, due to the large dimension of the city, and consequent high demanding computational resources. Concerning the Haiti study case, after the earthquake of 2010, the neighbourhood of Le Saline in Port au Prince (Haiti) has been investigated in depth and high-resolution DSM and building layers have been generated and made freely available.

For each selected city, Table 1 presents a schematic representation of the associated climate scenarios and summarizes the main features: study area, surface of green areas, as well as flat and sloped roofs according to the approach described in Section 3 for the roof identification. The total number of identified roofs is also included in Table 1, highlighting the percentage of flat and sloped roofs. The weather stations listed in Table 1 are used as references for both rainfall and temperature time series, which are then used to estimate the runoff generation in the investigated areas. Moreover, the 95%-quantile of the non-zero rainfall time series of each location, h_{95}, has been included in Table 1. This value has been selected as the threshold to define extreme rainfall events.

The geographical location of the selected cities is illustrated in Figure 1(a). For each city we defined a boundary with the aim to investigate urbanized areas, focusing on the historical centres, where the population density is usually higher. Study areas were also drawn considering data availability and thus do not overlap with the administrative boundaries: since our interest focuses on densely urbanized areas, isolated houses are not included in the study, and for most locations analysis is restricted only on the city centres. Figure 1 (b-s) shows selected city boundaries and a small-scale detail for each city, depicting the urban texture and the alternation of flat (green) and sloped (blue) roofs.

2.2. Climatological input: rainfall and evapotranspiration data

Rainfall and temperature time series, required for the hydrological simulations, were derived from the Global Historical Climate Network (GHCN) (Menne et al. 2012) at daily scale. For each city, the closest weather station with at least 25 years of precipitation and temperature observations was selected as the reference: the chosen GHCN weather station code and length of the time series are provided in Table 1. Time series lengths vary from a minimum of 26 years (for Auckland) to a maximum of 79 years (for Montreal). GHCN rainfall data are provided with a daily temporal resolution, which is a reasonable time step for simulation aimed at characterizing GR retention capacity, i.e. capacity of storing water that will be lost through evapotranspiration (Hellies, Deidda, and Viola 2018; Viola, Hellies, and Deidda 2017). Since an hourly or a finer temporal scale is generally required to investigate the runoff generation in urban areas (Cristiano et al. 2019; Ochoa-Rodriguez et al. 2015) and the detention capacity (i.e. capacity of storing water that will be released to the drainage network or used for other purposes after the rainfall event), we adopted a simplified approach (see Section 3.4) to investigate the benefits of the blue-green solution installation for sub-daily rainfall events.

Temperature data derived from the GHCN weather stations are also available at daily temporal resolution and they have been averaged at monthly scale to estimate the potential evapotranspiration with the Thornthwaite equation (Thornthwaite 1948).

3. Methodology

The approach adopted here to investigate the potential impact on runoff generation reduction achievable with a large-scale installation of blue-green solutions in urban areas is presented in the following. Section 3.1 describes the investigated blue-green solutions, i.e., extensive and intensive GRs, MBGRs and RWH systems, and their estimated costs. In Section 3.2, the methodology developed to identify the roof slope, and consequently the most suitable solution, is illustrated. Section 3.3 and 3.4 introduce the different investigated scenarios and the

Table 1. Characteristics of the investigated locations. Table includes surface and number of roofs for the selected areas and indications regarding the Global Historical Climate Network (GHCN) weather station names and duration of the rainfall and temperature time series selected for each location (described in Section 2.2) .

	London	Waterloo	Montreal	Port Au Prince	Airdrie	Cagliari	Auckland	Wellington	Vancouver
ID	A1[1]	A2[2]	A3[3]	B1[4]	C1[5]	D1[6]	D2[7]	D3[8]	D4[9]
Climate Case (R / ET)									
Investigated Surface [ha]	208144	6324	54052	52	2607	2966	74418	5715	11074
Green Areas [ha]	80783	853	3912	7	421	299	10865	957	946
Surface Flat Roofs [ha]	2293	254	7833	4	209	86	1686	82	520
Surface Sloped Roofs [ha]	22528	634	3735	16	161	455	8050	828	1555
N Roofs	726217	41150	358576	5508	19658	7978	506602	53699	120767
% Flat Roofs	14	5	56	23	55	13	4	3	9
% Sloped Roofs	86	95	44	77	45	87	96	97	91
Weather Station Code	UKE001 05915	USC0030 6047	CA007025 250	DRM000 78482	CA 003031093	421300	NZM000 93110	NZ0000934 17	CA001108 395
Time series Length [year]	57	38	79	47	32	56	26	33	43
h_{95} [mm]	9.7	14.7	15	26.9	6.6	7	15.2	14.7	17

[1]https://data.gov.uk/dataset/fba12e80-519 f-4be2-806 f-41be9e26ab96/lidar-composite-dsm-2m, https://data.gov.uk/
[2]http://ftp.maps.Canada.ca/pub/elevation/dem_mne/highresolution_hauteresolution/dsm_mns/1m/, http://data.waterloo.ca/
[3]http://ftp.maps.Canada.ca/pub/elevation/dem_mne/highresolution_hauteresolution/dsm_mns/1m/, http://donnees.ville.montreal.qc.ca/dataset
[4]http://opentopo.sdsc.edu/datasets?minX = −74.2499957084656&minY = 16.299044835995616&maxX = −71.01562714576725&maxY = 20.96143360280668, https://data.world/hot/65a41adf-1068-4964-be4c-08f435e5d302
[5]http://ftp.maps.Canada.ca/pub/elevation/dem_mne/highresolution_hauteresolution/dsm_mns/1m/, http://data-airdrie.opendata.arcgis.com/
[6]http://www.sardegnageoportale.it/
[7]https://data.linz.govt.nz/
[8]https://data.linz.govt.nz/
[9]http://ftp.maps.Canada.ca/pub/elevation/dem_mne/highresolution_hauteresolution/dsm_mns/1m/, https://data.vancouver.ca/datacatalogue/

approach followed to estimate the runoff reduction and the delay in the runoff generation from rooftops for each scenario.

3.1. Rethinking the role of city rooftops

To maximize the runoff mitigation performances of each solution (i.e. GR, MBGR and RWH system) and to guide the choice between these tools, the available roof surfaces are exploited to detect flat and sloped roofs. The former ones are, indeed, more suited for GR or MBGR installation, while the latter can be more convenient for the RWH systems. Following the definition proposed by Santos, Tenedório, and Gonçalves (2016), roofs can be classified as 'flat' if their average slope is less than 11°. Conversely, we refer to 'sloped roof' when the average slope is more than 11°.

This threshold choice is functional to GR and MBGR installations, which are generally easier, less expensive and more efficient in terms of retention capacity on flat roofs (Villarreal and Bengtsson 2005; Czemiel Berndtsson 2010). Although RWH systems could also be installed on flat roofs, our study does not include this option, with the aim of emphasizing the GR and MBGR multisectoral additional benefits in the sustainable urban development. Moreover, we aim to maximize the mitigation capacity by installing the more efficient solution, and, as it will be shown in Section 4.1, at building scale, GRs and MBGRs present higher performances.

Furthermore, two different options regarding GRs are evaluated: extensive and intensive structures. Extensive GRs are characterized by a soil layer generally thinner than 15–20 cm

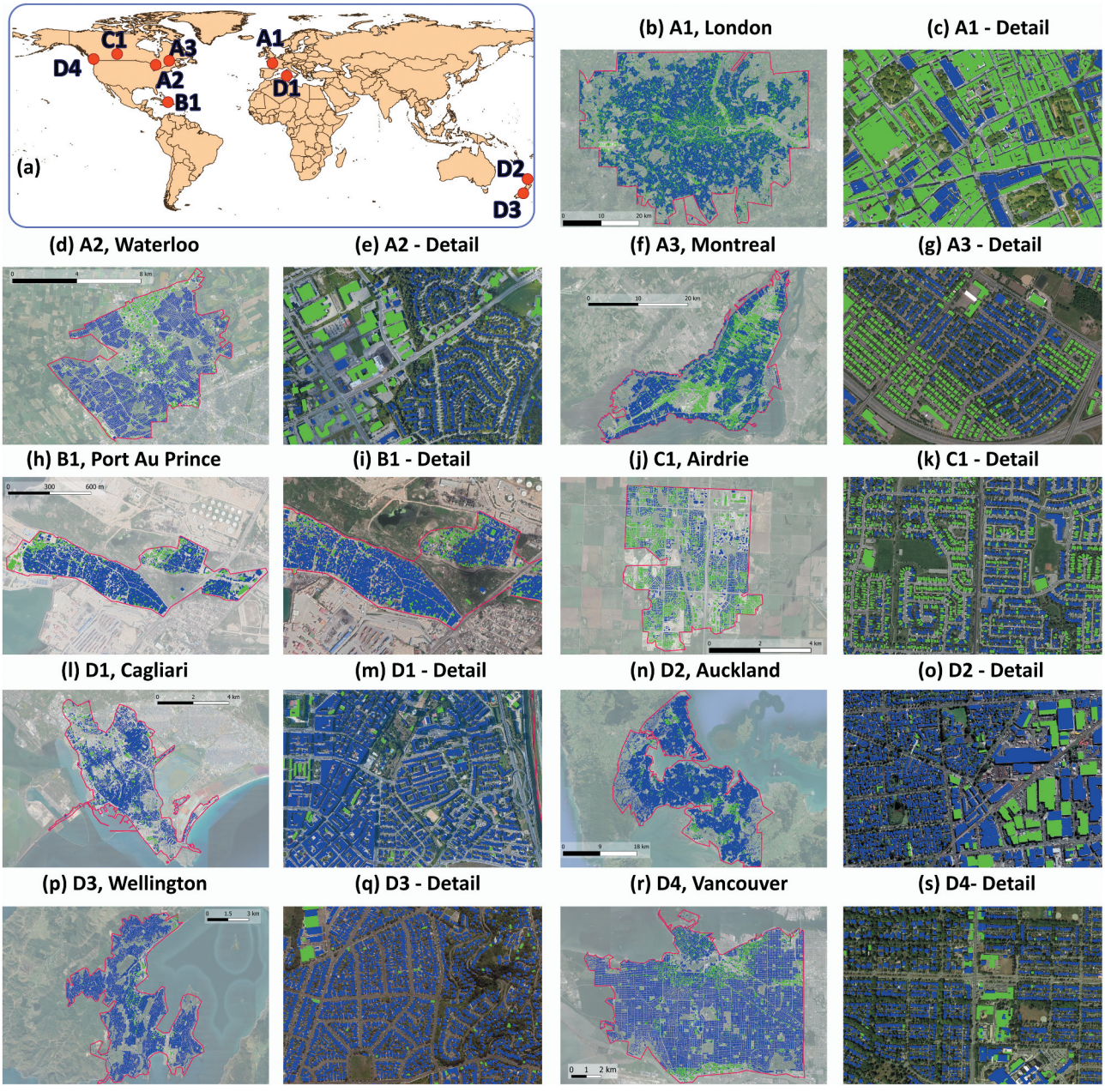

Figure 1. (a) Location of the 9 selected case studies described in Table 1. Boundaries (b, d, f, h, j, l, n, p, r) and details (c, e, g, i, k, m, o, q, s) of the case studies are illustrated with flat roofs highlighted in green, while sloped roofs are represented in blue. Flat and sloped roofs are classified following the approach described in Section 3.

where grass or shallow-root vegetation is placed; intensive GRs, instead, present a thicker soil, which allows the plantation of trees and shrubs. Extensive GRs are more flexible, easier to install and less expensive than intensive ones in terms of both construction and maintenance costs. To evaluate the cost-efficiency of these two options, in this work we analysed the installation of extensive and intensive GRs with a soil thickness of 15 cm and 30 cm, respectively. Silty loam soil, with a porosity of 50%, is assumed to characterize both extensive and intensive GR (Clapp and Hornberger 1978).

Installation costs of GRs depend on the roof extension: based on literature a unitary cost of 100 euro/m^2 is assumed for extensive GRs, while 250 euro/m^2 for intensive ones (Bianchini and Hewage 2012; Mahdiyar et al. 2016; Feng and Hewage 2018; Rosasco and Perini 2019).

To limit the potential weight of MBGRs on the roof, the soil layer is usually thin, with a maximum thickness of 15 cm, like the one of extensive GRs. Hence, only grass or shallow-root vegetation can be planted. The water storage layer is usually 8–10 cm thick. The average unitary cost of a MBGR, including installation and maintenance amortised at the time of construction, is around 230 euro/m^2 (https://metropolder.com/en/).

In a similar way, RWH system mitigation performance is evaluated through the installation of tanks. Tank costs depend on the chosen volume, and for the investigated cases a reasonable unitary cost can be assumed equal to 170 euro/m^3, deriving this value from commercial catalogues. These

unitary costs include the installation costs and the maintenance costs amortised at the time of construction.

3.2. Roof detection: slope and area analysis

Automatic identification of roofs and slope calculation are fundamental steps to choose the more suitable flood mitigation solution to be installed. In this work, we present a simple and fast approach to individuate roofs and estimate their slope and area, combining maps with building shape layers and Digital Surface Model (DSM). Both these data are generally freely available at high resolution for many municipalities. The building shape layer provides polygons of urban buildings, and it is used first to identify the roofs within a city. It is worth mentioning that in the case of detached houses a single polygon coincides with a unique casing, while for denser urban fabric a single polygon may contains several rooftops. The building shape layer serves as mask to single out the DSM pixels belonging to the roof. For each pixel, the slope is calculated in relation to the 8 surrounding pixels and the maximum slope is then selected. To estimate the slope of each roof, the slope of all the pixels belonging to the selected building is averaged over the total roof surface, detected from the building mask. To avoid boundary errors, single pixel slopes larger than 45° were excluded from the study. Figure 2 describes the approach followed to identify the average slope of each roof and consequently the flood mitigation solution that is selected in this study.

Pixel resolution plays a significant role in this analysis and reliable results are achievable with DSM resolution higher or equal to 2 m. A coarser resolution would increase the uncertainties in the identification of the single roof area and slope.

It should be mentioned that the above approach implies that all the roofs would be suitable for our purposes, without structural or architectural impediments. This hypothesis is unlikely, especially in old cities, and for this reason, we performed our analyses explicitly considering a varying percentage of implementation of green and blue solutions within each city.

3.3. Retention efficiency analysis under different blue-green scenarios

In our analysis, the following scenarios have been simulated, considering different combinations of GR, MBGR and RWH systems:

(a) no intervention,
(b) extensive GRs over flat roofs,
(c) intensive GRs over flat roofs,
(d) MBGRs over flat roofs
(e) RWH systems under sloped roofs,
(f) combination of RWH systems for sloped roofs and extensive GRs on flat ones,
(g) combination of RWH systems for sloped roofs and intensive GRs on flat ones,
(h) combination of RWH systems for sloped roofs and MBGRs on flat ones.

Many approaches are available in literature to estimate the runoff generation and the total outflow in an urban catchment. The main difficulties in modelling runoff in urban areas are related to their complex geometry and heterogeneity: many semi and fully distributed models have been proposed (see e.g. Aronica and Cannarozzo (2000), Pina et al. (2016), Gires et al. (2018) among the others), but most of them require a long computational time and spatially and temporally distributed data (Pina et al. 2016). Even when conceptual models are used (see for instance the one developed by Cristiano, Deidda, and Viola (2020)), parametric uncertainties constitute an impediment to the clear interpretation of the results. Since the aim of this work was to obtain a fast estimation of the total discharge from urban basin, a conceptual simplified model was selected. The rational method proposed by Kuichling (1889) was chosen to estimate the total discharge Q_0 [m^3/day] for scenario (a), corresponding to 'no intervention':

$$Q_0 = \psi i A * 10, \tag{1}$$

where i is average rainfall intensity over the area at daily scale [mm/day], A [ha] indicates the total urban watershed area and ψ [-] is the runoff coefficient. The term φ, which is the only

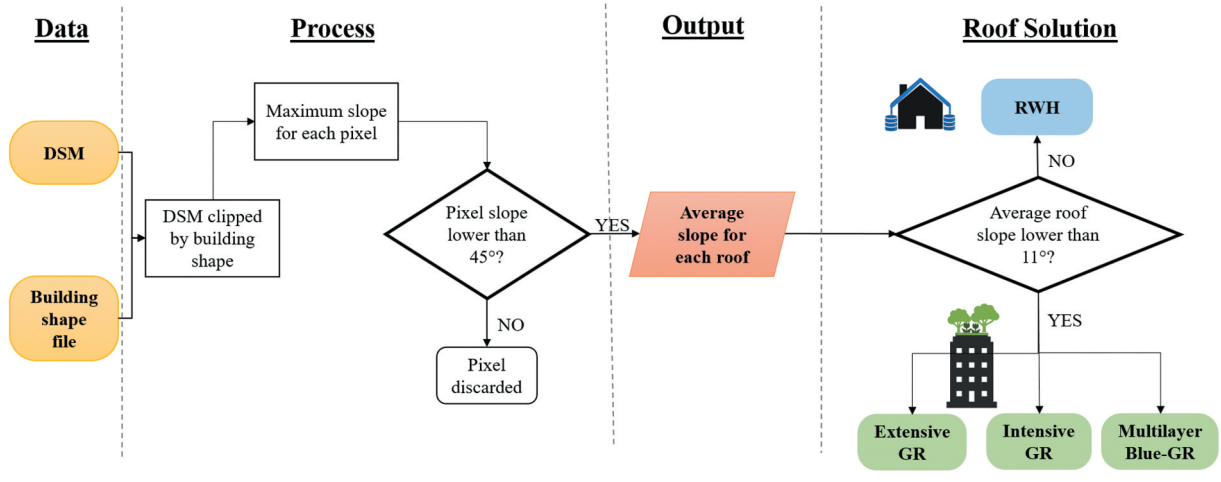

Figure 2. Flowchart representing the approach adapted to identify the average roof slope and the most suitable flood mitigation solution selected for our study.

model parameter and thus incorporates all the uncertainties, is estimated as weighted average of the imperviousness coefficients $\psi_{\#}$ associated with each category of land use of total extension $A_{\#}$. In our study, we partition the total urban areas into green areas (A_G, ψ_G), building rooftops (A_B, ψ_B) and roads $(A_R, \varphi\psi_R)$, obtaining:

$$\psi = \frac{A_G\varphi_G + A_B\psi_B + A_R\psi_R}{A} \tag{2}$$

Commonly used values of imperviousness coefficients are derived from literature: ψ_G is assumed equal to 0.2, ψ_B is set equal to 1 and ψ_R to 0.9 (Becciu and Paoletti 2000).

The installation of GRs on rooftops mitigates the runoff generated from the building because, during rainfall events, the soil layer in GRs retains a certain volume of water that will be absorbed by the vegetation roots and released to the atmosphere through evapotranspiration on a much larger time scale. In this work, the GR mitigated discharge Q_{GR} for scenario (b) and (c) is estimated with the Ecohydrological Streamflow Model (EHSM) presented by Viola, Pumo, and Noto (2014), that simulates the hydrological behaviour of such a GR installation. This parsimonious conceptual model, based on water balance, uses local rainfall time series and potential evapotranspiration series as climatological input and can be adapted to represent the GR behaviour and to estimate the mitigated discharge Q_{GR} (Viola, Hellies, and Deidda 2017; Hellies, Deidda, and Viola 2018). The EHSM describes the GR as a combination of a soil bucket and two parallel linear reservoirs, employing four main parameters to describe the soil and vegetation characteristics: the active soil depth (nZ_r) is derived from the product of soil depth Z_r and porosity n, the field capacity (S_{fc}), i.e. the soil moisture values when leakages begin, and the hygroscopic point (S_u), i.e. when the soil starts retaining water, and the vegetational coefficient (K_c), which is assumed as in standard condition equal to 1. The soil is assumed as silty loam and the parameters Z_r, S_{fc} and S_u are consequently derived from literature (Laio et al. 2001; Clapp and Hornberger 1978). As mentioned in Section 3.1, the soil layer depth Z_r is set equal to 15 cm for extensive GRs and to 30 cm for the intensive configuration (i.e. scenarios (b) and (c), respectively).

Similarly, the installation of RWH systems ensures a reduction in the runoff generation, since it enables water to be collected from rooftops and stored in tanks. The choice of the tank volume depends on the expected rainwater volume and on the detention capacity the designer wants to achieve, and it is constrained by the space available for the installation. For each sloped roof j, we hypothesized to install a tank that can store a volume $V_{tot,j}^{RWH}$ [m^3] equal to the daily discharge generated from the sloped roof surface $A_{S,j}$ [m^2] during a reference extreme event. Specifically, the 95%-quantile of the cumulative probability distribution of daily rainfall time series h_{95} (Table 1) was selected as the reference for rainfall depth, meaning that the storage volume capacity is being estimated for peak rainfall events. For each investigated location, the total storable volume, V_{tot}^{RWH}, is hence defined as:

$$V_{tot}^{RWH} = \sum_{j=1}^{N_S} (A_{S,j} * h_{95}) \tag{3}$$

where N_S is the number of sloped roofs detected in the city.

The water collected during rainfall events, if properly stored and treated, can be reused for domestic non-potable purposes, such as garden irrigation and toilet flushing. In order to simulate these potential withdrawals, it is assumed that a small percentage of the volume, namely 10%, is used every day. It follows from this assumption that water volume within the tank linearly decays if no rainfall event occurs. The daily mitigated discharge Q_{RWH} [m^3/day], in case of large-scale RWH tank installation, as in the scenario (e), can be derived from a simple mass-conservation equation, subtracting from the unaltered outflow Q_0 the daily collected water volume in all the tanks installed. If the tank at the day $i-1$ is empty and the rainfall depth at the day i is lower than h_{95}, all the rainwater is stored in the tank and $Q_{RWH} = 0$, otherwise an outflow $Q_{RWH} \leq Q_0$ may occur. The water level in the tank is hence included in the model as a status variable, since it allows how much volume is available each day to eventually store rainwater to be estimated.

MBGR response to rainfall inputs, which is required for scenario (d), is estimated by coupling the GR and the RWH models. Therefore, we combine an extensive GR, simulated with the ecohydrological model previously described, leaking into an additional storage layer, modelled as the RWH tank with a simple mass conservation. The same vegetation and soil parameters as those chosen for the extensive GR are also selected for the MBGR, while the additional storage layer is assumed to have the same extension of the GR soil layer and to be 8 cm deep. As for the RWH tanks, a daily potential withdrawal of 10% of the total volume is considered, accounting for evaporation and potential reuse of the collected water.

Retention capacity is evaluated through the potential discharge reduction ΔQ_*, which is defined for each scenario as the difference between the unaltered discharge Q_0 and the mitigated discharge $Q_*(* = GRorRWH)$, relative to the unaltered conditions:

$$\Delta Q_* = \frac{Q_0 - Q_*}{Q_0}. \tag{4}$$

3.4. Time between rainfall and runoff generation from rooftops

Besides the retention capacity, discussed in Section 3.3, the three blue-green solutions investigated in this work are recognized for their detention capacity, i.e. the ability to increase the time between rainfall and runoff generation from the building. Due to the presence of GRs, MBGRs and RWH systems, indeed, the runoff generation from rooftops starts when the soil moisture in the GR reaches the leakage triggering point or when the RWH tank is full, while for MBGR both conditions must occur. With the aim to investigate the benefits of the installation of blue-green solutions in urban areas, the runoff generation delay, T_{lag}, has been estimated and discussed for both tools.

T_{lag} strongly depends on the antecedent conditions of the blue-green solution and on the duration and intensity of the rainfall event. As described in Section 2.2, rainfall data in this

study were only available at daily resolution, whereas higher temporal resolutions are required to assess the hydrological response in an urban catchment (Cristiano et al. 2019). For this reason, we investigated the response of GRs, MBGRs and RWH systems assuming the worst conditions, i.e. synthetical events characterized by the same daily rainfall depth R uniformly distributed on smaller durations τ (from 1 to 24 h). The rainfall intensity R_τ for each duration τ is thus calculated dividing the daily rainfall depth by τ, e.g. in the case of τ = 1 h, the rainfall is falling only in the first hour with a rainfall intensity $R_1 = \frac{R}{1h}$; for τ = 3 h rainfall intensity is $R_3 = \frac{R}{3h}$ and so on. For τ = 24 h, the event is assumed to be uniformly distributed during the whole day. For each day i and for each considered duration τ it is possible to identify the volume per unit of roof surface $h_{lag_{i,\tau}}$ that has to be filled before the runoff generation begins:

$$h_{lag_{i,\tau}} = \begin{cases} (S_{fc} - S_{i-1})nZ_r & \text{for GRs} \\ (S_{fc} - S_{i-1})nZ_r + \left(\frac{V_{tot}^{MBGR} - V_{i-1}^{MBGR}}{A_f}\right) & \text{for MBGRs} \\ \frac{V_{tot}^{RWH} - V_{i-1}^{RWH}}{A_s} & \text{for RWH systems} \end{cases} \quad (5)$$

It is worth recalling that the term S_{fc} (i.e. the field capacity) represents the soil moisture values triggering the leakage, S_{i-1} indicates the soil water content at the $i-1$ day, n is the porosity and Z_r is the soil depth. The terms V_{tot}^{MBGR} and V_{tot}^{RWH} indicate the maximum storable volume of all the potentially installed MBGRs and RWH tanks, respectively, while V_{i-1}^{MBGR} and V_{i-1}^{RWH} are the volumes accumulated in the MBGR storage layers and in the RWH tanks at the $i-1$ day. A_f and A_s are the total area of flat and sloped roof, respectively connected to MBGR or to the tank in the investigated area.

The runoff generation delay, T_{lag_τ} can be finally defined as:

$$T_{lag_\tau} = \begin{cases} \frac{h_{lag_{i,\tau}}}{R_\tau} & \text{if } h_{lag_{i,\tau}} \leq R_\tau * \tau \\ +\infty & \text{if } h_{lag_{i,\tau}} > R_\tau * \tau \end{cases} \quad (6)$$

Under the first condition, eq. 6 provides a runoff generation delay $T_{lag_\tau} \leq \tau$, thus there will be runoff generation from the investigated solution as a consequence of a certain rainfall event. Conversely, under the latter condition, the adopted solution assures, for the considered event, an ideal condition of no runoff generation from rooftops, since all the rainwater is retained by the infrastructure.

4. Results and discussion

This section presents and discusses the results obtained following the approach described in Section 3. In Section 4.1, the analysis is developed at building scale, focusing on the retention capacity of the single blue-green solution and the delay between rainfall and runoff generation from the rooftop that can be achieved. Subsequently, in Section 4.2, the impacts of a large-scale implementation are estimated, evaluating the roof slope distribution in each selected city and the potential discharge reduction in the different scenarios. Finally, a cost-efficiency analysis is presented in Section 4.3 enabling the comparison of costs and efficiency of the multiple scenarios of blue-green solution installation.

4.1. Analysis at building scale: retention capacity and delay in runoff generation

Following the assumptions and approach described in Section 3.3, it is possible to assess the storage capacity of extensive and intensive GRs, MBGRs and RWH systems. For a benchmark GR flat surface, A = 100 m^2, the maximum retention capacity C_{GR} (i.e. assuming that the soil is completely dry) is equal to: $C_{GR} = (S_{fc} - S_u) * A * nZ_r$, where n Z_r is the active soil depth, S_{fc} is the leakage triggering point, which corresponds to the field capacity, and S_u is the hygroscopic point, as already defined. Assuming a sandy loam as soil layer, and consequently $S_{fc} = 0.52$, $S_u = 0.11$, $n = 0.5$ (Laio et al. 2001), and a soil depth Z_r of 150 mm and 300 mm, the retention capacity C_{GR} is equal to 3 m^3 and 6.15 m^3 for extensive and intensive GRs, respectively. This means that it is possible to retain 30 mm and 61.5 mm rainfall depth in extensive and intensive GRs, respectively.

Similarly, the maximum retention capacity of a MBGR can be estimated as the sum of the maximum retention capacity of an extensive GR (C_{GRex}), i.e. when the soil is completely dry, and the maximum detention capacity of the storage layer (C_{SL}), i.e. when it is completely empty. Assuming a flat surface A = 100 m^2, and a storage layer thickness of 8 cm, the maximum storage capacity C_{MBGR} can be calculated as: $C_{MBGR} = C_{GR} + C_{SL} = 11m^3$. This volume corresponds to 110 mm of rainfall that can be stored at building scale. This value is quite high if compared to the 95%-quantile of the non-zero rainfall time series, h_{95}, reported in Table 1 for the 9 investigated locations, and which defines in this study the extreme rainfall events, suggesting that MBGRs can potentially retain almost all the rainfall events.

For the RWH systems, the maximum retention capacity is achievable when the tank is empty and corresponds to the tank volume, which is assumed to be a function of h_{95} (see Section 3.3), characteristic of each location (Table 1). Considering a benchmark sloped surface, A = 100 m^2, the tank volume is given by $C_{RWH} = A * h_{95}$, as defined in Section 3.3. Across the investigated locations, C_{RWH} varies between a minimum of 0.66 m^3 (Airdrie, C1) and a maximum of 2.7 m^3 (Port Au Prince, B1), corresponding to about 7 mm and 27 mm rainfall depth, respectively.

Summarizing, for a 100 m2 roof, the retention capacity for extensive and intensive GR is equal to 3 m^3 and 6.15 m^3, for MBGR it rises to 11 m^3, while if a RWH system is installed, the maximum storage capacity varies between a minimum of 0.66 m^3 and a maximum of 2.7 m^3, depending on the investigated location. Comparing the retention capacity of extensive and intensive GRs and MBGRs with the storage capacity of RWH tanks, it is clear that in all the investigated locations, MBGRs and GRs present higher potential mitigation capacity than RWH systems at building scale.

In Section 3.4, we introduced a variable describing the delays in runoff generation from the rooftop at building scale.

T_{lag_τ} has been evaluated for extensive and intensive GRs, MBGRs and RWH systems, for the 9 selected locations.

Figure 3 illustrates the complementary cumulative distribution function (CCDF) of the time between rainfall and runoff generation from the rooftop, T_{lag_τ}, considering extreme rainfall events, namely all the event with depth higher than h_{95} : colours highlight the CCDF corresponding to different rainfall duration τ = 1, 3, 12 and 24 h, while the x-axis is limited to the range 0–5 h, to visualize better the response time characteristic of an urban catchment, which is generally of the order of or smaller than 1 h (Ochoa-Rodriguez et al. 2015). For high durations τ, the corresponding rainfall intensity R_τ decreases and the time between rainfall and runoff generation from building T_{lag_τ} increases. To help the reader in interpreting these plots, it is worth noticing that the higher the curve, the better the performances in terms of peak delay. Indeed, if, for a certain duration τ, the CCDF is close to 1 there is a high probability that the release of water from the considered GR or RWH system will start after the rainfall event or that no runoff will be generated at all. As a result of our analysis, the MBGR outperforms GR and RWH systems on delaying runoff generation. Indeed, the CCDF for each considered duration of the MBGR T_{lag_τ} is almost always equal to 1, since almost all the events are fully retained at building scale by the MBGRs. Thus, for a better readability of Figure 3, CCDF of MBGR are not included in the plots. Moreover, since MBGR demonstrated to be able to store the whole rainfall volume for almost all the considered events, being an ideal solution, the following discussion will be limited to the other two considered systems only (GRs and RWH systems).

In all locations, the CCDFs for RWH systems start from 1, highlighting that all the events with intensity higher than h_{95} present at least a small delay in the runoff from the building. This is due to the hypothesized RWH system design characteristics that ensure that the empty tank can retain events with rainfall depth equal to h_{95} and that 10% of the volume is used daily for domestic purposes (See Section 3.3). The latter guarantee a quick emptying of the tank (faster than soil drying) and thus the existence of a volume, albeit small, for storing rainfall. On the other hand, both extensive and intensive GRs, present CCDFs with the maximum lower than 1, meaning that

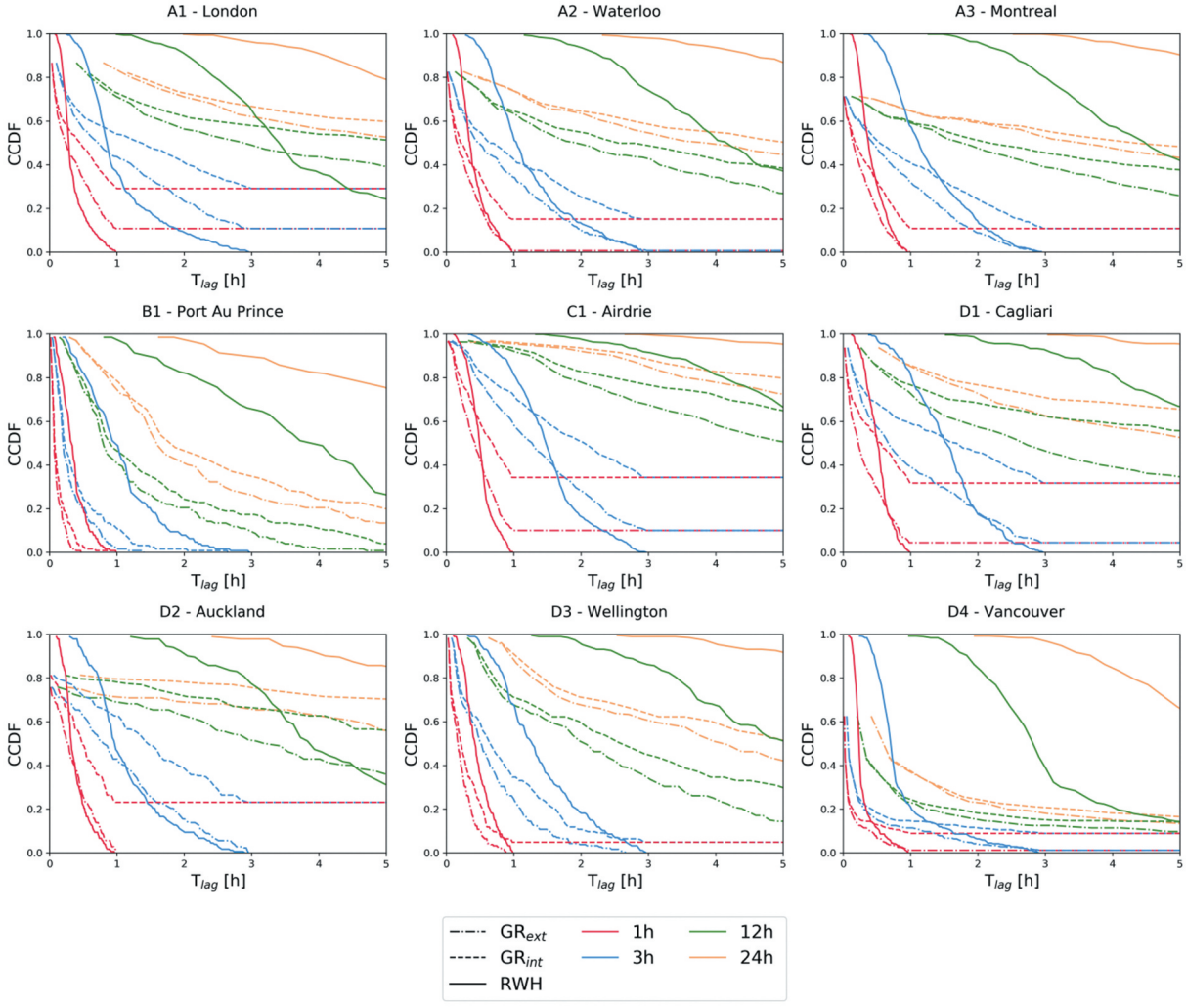

Figure 3. Complementary cumulative distribution function (CCDF) of T_{lag} for the 9 investigated locations. Different colours indicate the probability distribution related to different rainfall durations (1 h, 3 h, 12 h, 24 h). The three investigated solutions (extensive and intensive GRs and RWH systems) are highlighted with a different line style. The x-axis is limited to the range 0–5 h.

some extreme events are not even partially retained by the green solution. This is related to antecedent soil moisture conditions: in fact, if rainfall occurs on saturated soil there is no space for water storage and thus runoff is immediately generated. GRs also show an opposite behaviour: namely there is a horizontal line representing the probability of not generating runoff.

Let us see, for example, the case of an intensive GR installed in Waterloo (A2): the maximum value of the CCDF of T_{lag} for events with duration 1 h (dashed red line in Figure 3) is equal to 0.8, indicating that 20% of the extreme 1-hour events are not retained at all and runoff occurs immediately when rainfall began. On the other hand, almost 15% of 1-hour events do not generate runoff, as is highlighted by the horizontal line. This is the case of extreme rainfall events occurring when soil moisture is low and thus there is enough volume to store incoming water.

A relevant exception is represented by Port au Prince (B1), where the climatic conditions are characterized by high annual precipitation and intense rainfall events ($h_{95} = 27mm$, see Table 1), with a consequently lower capacity of storing water in the soil on a generic day of the year. This is the reason why this city is the only one without a horizontal line in the CCDF, even for the intensive GR configuration.

Overall, considering intensive GR and rainfall events with $\tau = 1h$ (dashed red lines in Figure 3), there is no runoff generation from the rooftops in the first hour for a percentage of events that varies between 5% (Wellington, D3) and almost 40% (Airdrie, C1). With the installation of an extensive GR, instead, the percentage of extreme rainfall events that do not generate runoff from the rooftops is lower, with a maximum in Airdrie (C1) and London (A1), of almost 15%, and it is null in many locations (A2, A3, B1, D2 and D3). If we consider short response time, less than 30 min, and extreme rainfall events with $\tau = 1h$ (red lines if Figure 3), RWH systems generally ensure a high probability not to generate runoff from rooftops.

4.2. Analysis at large urban scale: roof distribution and long-term simulation

As a preliminary step for the evaluation of the potential installation benefits of combined green blue infrastructures, we investigated the flat and sloped roof distribution and their extensions in each considered city. Such analysis revealed a high variability among the cities, depending on neighbourhood, construction tradition and in some way on climate (steep roofs, for instance, are typical of snowy places).

The histograms plotted in Figure 4 illustrate, for the nine selected locations, the area frequency distribution of flat (less than 11°, green) and sloped (more than 11°, blue) roofs: the surfaces generally vary from 20 to a few hundred square metres (up to 5000 m2 in rare cases), with noticeable differences in their distribution from city to city. The presence of very large roofs in the cases of London (A1) and Cagliari (D1) is related to the peculiar urban fabric: both present, in fact, contiguous buildings, which are considered as a single unit in the GIS layer. However, it is worth noticing that such peculiarities do not affect the analyses presented in this work.

Although with some small differences, the 9 investigated cities present right-skewed distribution of sloped roofs (blue) with a modal value around 150 m2. Port au Prince (B1) represents an exception: the average roof dimension is smaller and most of the roof surfaces are lower than 100 m2. This is due to the fact that this study is limited to a residential neighbourhood in the historical centre, where single buildings are generally very small. In some locations (Waterloo (A2), Airdrie (C1), Auckland (D2) and Wellington (D3)) the distribution of sloped roof presents a second peak for very small roofs, around 50 m2.

Except for Montreal (A3) and Airdrie (C1), sloped roofs are generally more frequent than flat ones, as already reported in Table 1. In the case of Waterloo (A2), Auckland (D2) and Wellington (D3), the number of flat roofs is smaller than the number of sloped ones, but the total surface covered by flat roofs is quite large. A common feature among the nine investigated locations is that sloped roofs are mainly detected above small properties and correspond to private houses, while large flat roofs correspond to public buildings or massive constructions, such as shopping malls (Figure 1 (c, e, g, k, m, o, q, s), see detail box of each location). This is clear in Waterloo (A2), where most of the large rooftops are located at the University campus (Figure 1 (e), detail box of Waterloo), while small, sloped roofs characterize the residential area.

Montreal (A3) and Airdrie (C1) show a different behaviour, highlighting overlapping distributions for flat and sloped roofs. The number of flat and sloped roofs is similar, and the covered surface is comparable. In these two cases, the roof distribution can be explained by the presence of neighbourhoods with small-medium houses characterized by flat roofs (Figure 1 (g, k)).

Differences in the roof slope distribution in the selected locations highlight how climate and cultural and socio-economic factors can influence the building typology and roof slope and distribution. Similarities between Auckland (D2) and Wellington (D3) or between Airdrie (C1) and Montreal (A3) are attributable to a geographical proximity and to a similar socio-economic development. Understanding these patterns helps identify more efficient solutions to mitigate flood risk and, in general, developing smarter and more resilient cities.

Once the roof distributions in each city is depicted, we investigated the discharge reduction at daily scale, under the seven blue-green scenarios introduced at the beginning of Section 3.3. With this aim, we analysed the output of models described in the same Section 3.3, forced by local rainfall and evapotranspiration time series, derived from the GHCN weather stations listed in Table 1. Simulations allowed the analysis of the potential retention capacities of extensive and intensive GRs, MBGRs and RWH systems, considering single or coupled implementations. For each location, Figure 5 provides an example of a 20-day time window, centred in the maximum rainfall event recorded in the local GHCN rainfall time series, of the key variables involved in the study: rainfall depth, discharge in unaltered conditions (Q_0) and in the seven considered scenarios (Q_*). Moreover, the water level in a RWH tank and in a MBGR storage layer, estimated as the ratio of total rainwater volume collected in the all tanks or MBGRs normalised by the total

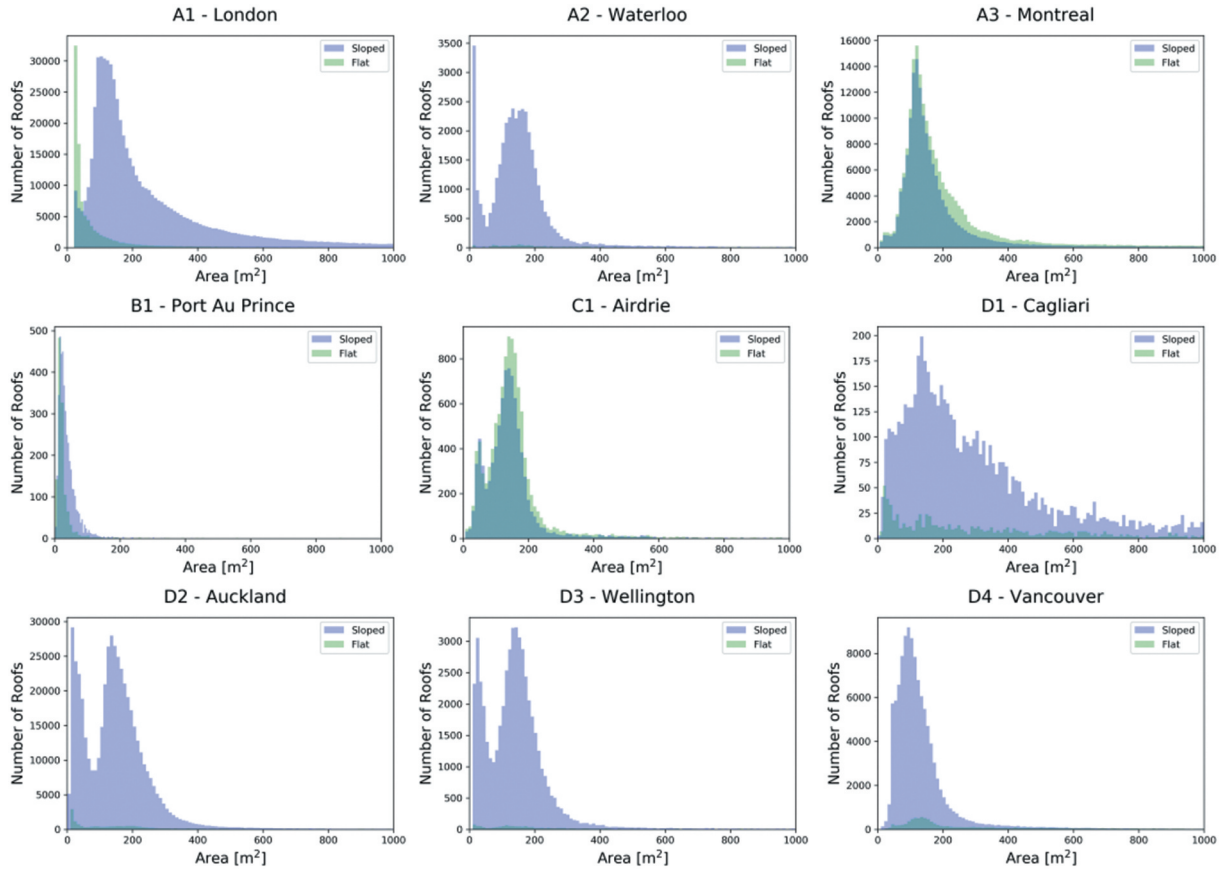

Figure 4. Flat and sloped roof area distribution histograms of the 9 locations. Roof area is limited at 1000 m^2 for graphical visualization.

sloped roof surface, are plotted on the secondary axis, with a purple and red dot-dashed line respectively.

Time series plotted in Figure 5 highlight the importance of the antecedent weather conditions. For example, mitigation performance of MBGRs depends on the water stored during previous days: if there are consecutive rainy days, stored water can reach the storage layer capacity, as in the example of Waterloo (Figure 5, A2) or Vancouver (Figure 5, D4), and the impact of MBGR on flood mitigation can be slightly limited. In other cases, as Cagliari (Figure 5, D1), Auckland (Figure 5, D2) or Montreal (Figure 5, D4), the water storage layer is often empty, ensuring a storage capacity for the incoming event. In this case the contribution of MBGRs in mitigating runoff is significant. Although the storage capacity is lower, similar considerations about the importance of antecedent weather conditions can be drawn observing the behaviour of the RWH tanks.

To focus better on extreme events, we investigated the retention capacity during days with rainfall depth higher than h_{95} (Table 1). For each extreme event, the discharge in unaltered conditions Q_0 and the discharge reduction ΔQ_* for the seven different scenarios of blue-green solution installation, as described in Section 3.3, have been estimated and are plotted in Figure 6 for the 9 investigated locations. Different colours and symbols highlight the seven different scenarios.

Thanks to their high retention and detention capacity, large-scale implementation of MBGRs always ensures a minimum runoff reduction of 2% in all investigated locations, with the best performance in Montreal (A3) and Airdrie (C1), where the minimum runoff reduction achievable with the installation of MBGRs at large-scale rises to 16% and 10% respectively due to the high density of flat roofs.

The combination of RWH and either intensive GRs or MBGRs always ensures the maximum flow reduction, that reaches 20% in most of the cases. Under the assumptions made in this study, the retention capacity at building-scale of GRs and MBGRs is larger than the one of RWH tanks, as argued in Section 4.1. When mitigation capacity is evaluated at large city scale, however, RWH systems show a better retention performance, due to the fact that, except for locations A3 and C1, the total area of sloped roofs is larger than flat ones in the analysed cities. For this reason, the maximum discharge reduction ΔQ achieved with the installation of RWH systems (Figure 6, dark blue symbols) is higher than the one achieved with GRs (Figure 6, dark and light symbols for extensive and intensive structures, respectively) or with MBGRs (Figure 6, light blue symbols). Montreal and Airdrie (Figure 6, A3 and C1) present an exception, since the percentage of flat roofs in both the cities (Figure 2) is comparable to the percentage of sloped roofs. In this case, the outflow reduction obtained with the GR or MBGR installation is higher than the one achieved with RWH systems.

Another general outcome of this comparative study is that when rainfall depth is higher than h_{95}, the potential efficiency of RWH and GRs gradually reduces as the magnitude of the rainfall events increases, while MBGRs ensure a constant performance for almost all the extreme rainfall events. Only in Port au Price (Figure 6, B1), where rainfall events are particularly

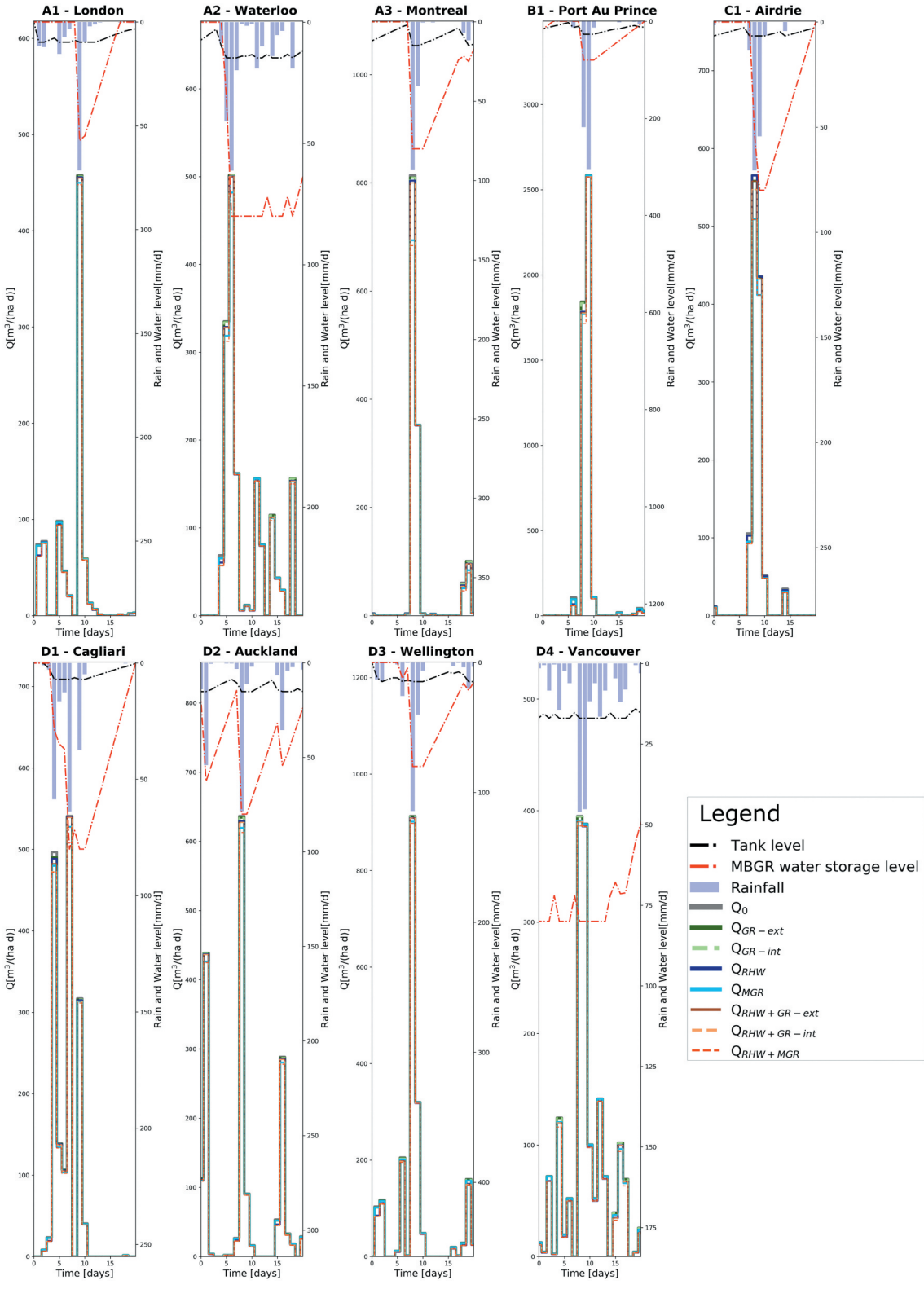

Figure 5. Example of the investigated time series. Total discharge is evaluated for the 8 different scenarios and plotted for a time window of 20 days, centred in correspondence to the maximum estimated unaltered discharge. With reference to the right-hand reversed axis, the purple dashed line and red dashed line represent the water level in the RWH tanks and in the storage layer of MBGRs, respectively and the bars in the upper part of the figures illustrate the rainfall time series.

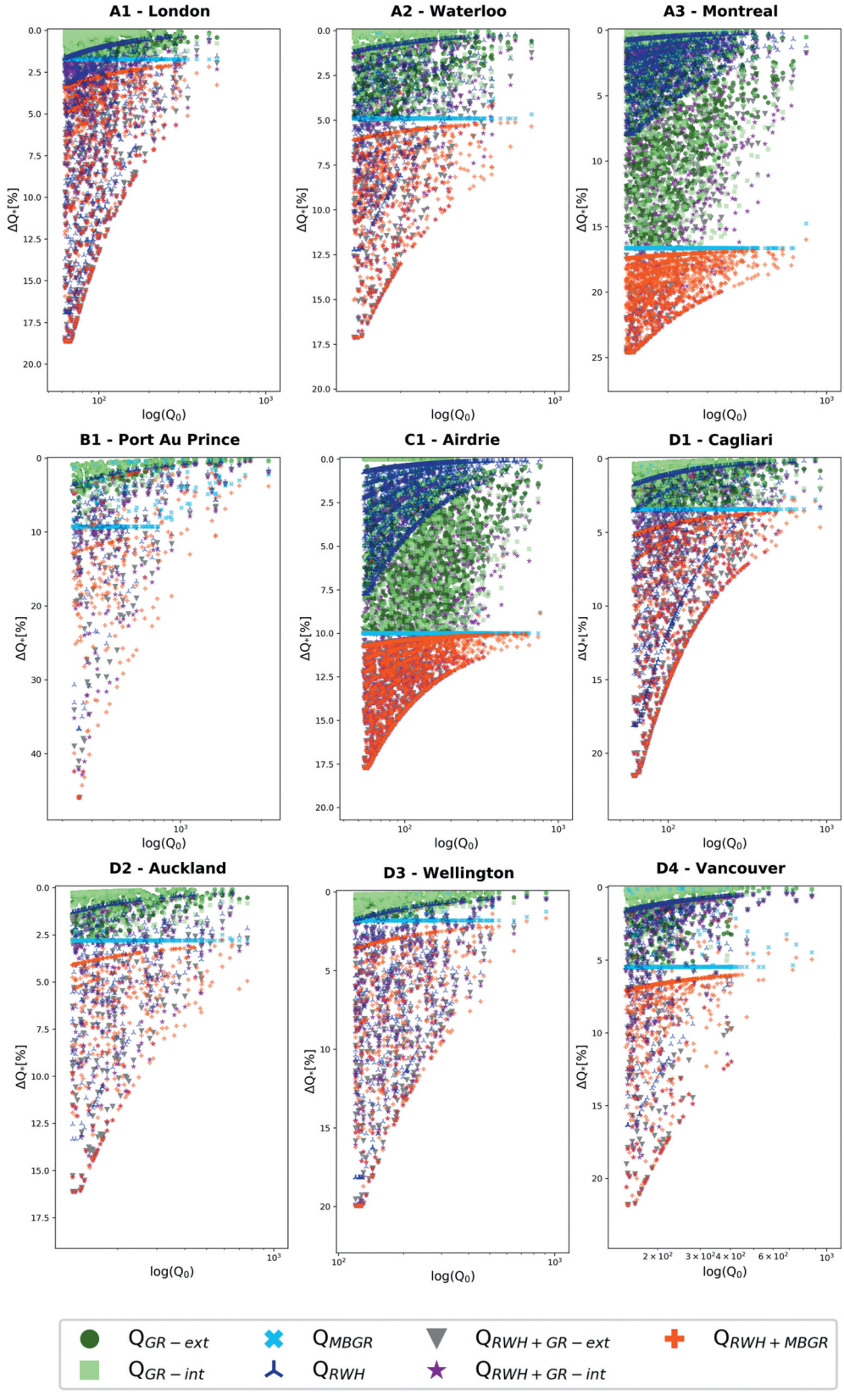

Figure 6. Outflow reduction at daily scale for different scenarios in the selected 9 locations in a semilogarithmic plot. Only the events with discharge in unaltered conditions above the 95% quantile are plotted.

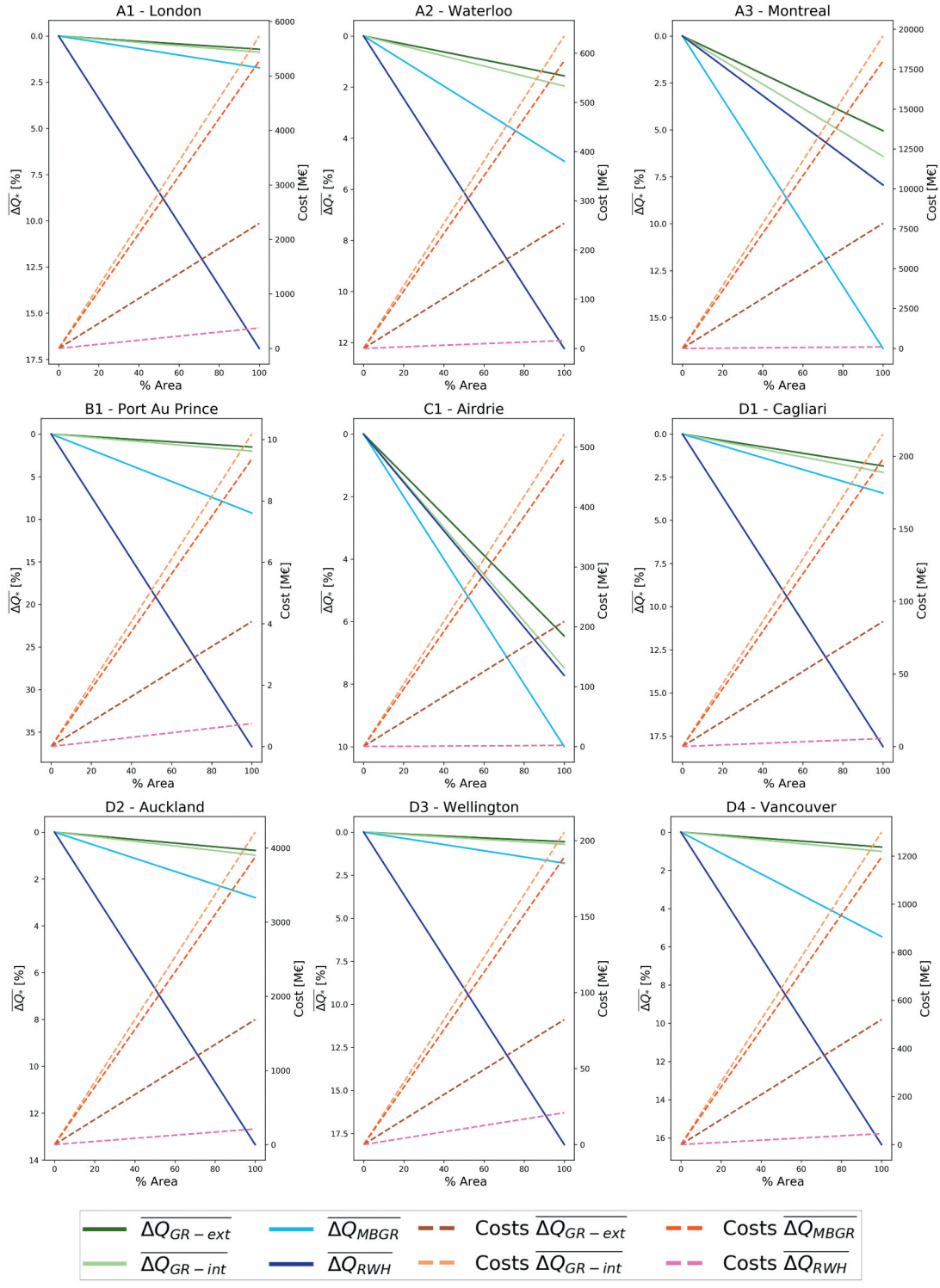

Figure 7. Effects of GR, MBGR and RWH installation over the entire city, for the 9 case studies. Potential discharge reduction $\overline{\Delta Q_*}$ (thick lines) and related costs (dashed lines) are plotted for extensive (dark green and dark brown) and intensive (light green and light brown) GRs, MBGR (light blue and Orange) and RWH (dark blue and pink), as function of the percentage of roof surface involved.

intense, the MBGR performance slowly decreases with the increase of rainfall depth. The high variability of discharge reduction ΔQ, which characterizes GRs and RWH systems, in correspondence to rainfall events with similar depth highlights the large influence of antecedent weather conditions on the retention and storage performance of these blue-green solutions. For the highest extreme rainfall events, we also observed that this variability decreases.

4.3. Cost-efficiency analysis

A cost-efficiency analysis to compare extensive and intensive GRs, MBGRs and RWH systems is presented in this section. To also evaluate the effects of partial implementation of such measures, discharge reductions and installation costs were determined for different percentages of the available flat and sloped roof areas (for potential extensive/intensive GR, MBGR and RWH system installation, respectively). In each considered city, we thus estimated the mean discharge reduction $\overline{\Delta Q}_*$, achievable with the installation of GRs, MBGRs and RWH systems for flat and sloped roof areas ranging from 0% to 100%, during the most critical rainfall events as:

$$\overline{\Delta Q}_* = \frac{\overline{Q_{095}} - \overline{Q_{*95}}}{\overline{Q_{095}}} \tag{7}$$

where $\overline{Q_{095}}$ and $\overline{Q_{*95}}$ are the mean discharge generation in unaltered conditions and in the different scenarios (* = GR, MBGR or RWH), calculated as average of all the discharge values originated by the events with rainfall depth higher than the 95%-quantile of the non-zero rainfall time series (h_{95}).

The cost-efficiency analysis is illustrated in Figure 7, where the total costs and mean outflow reduction are plotted as function of the percentage of available roof area that is potentially used for the installation: the left vertical axis refers to the benefit in terms of discharge reduction $\overline{\Delta Q}_*$ for each partial implementation, while the right vertical axis refers to the corresponding total costs, estimated by multiplying the unitary costs presented in Section 3.1 by the exploited area. Performance and costs of the coupled systems ($\overline{\Delta Q_{RWH+GR-ext}}$, $\overline{\Delta Q_{RWH+GR-int}}$ and $\overline{\Delta Q_{RWH+MBGR}}$) can be derived as the sum of outflow reduction and costs of GRs, MBGRs and RWH and are not included in Figure 7 to facilitate the visualization of cost-efficiency of the single structures.

Due to their thicker soil layer, intensive GRs guarantee a larger flow reduction than extensive scenarios. However, the difference between the extensive GR outflow reduction and the intensive one is small when one considers the city scale and seems not to justify a preference for the former to the latter in terms of costs. Only for Montreal (A3) and Airdrie (C1), the intensive configuration determines a considerable outflow reduction, that can motivate the large-scale installation of GRs. This happens since the flat roof percentage in both cities is quite high and it reaches almost 50% of the total roof surface.

Thanks to the additional storage layer, MBGRs ensure a runoff generation reduction more than double the one of GRs, while the total costs are almost the same as the installation of intensive GRs. However, as for the traditional GRs, the MBGR performance is limited by the lower percentage of flat roofs in most of the investigated cities. Only in Montreal (A3) and in Airdrie (C1), the flat surface available for MBGRs is enough to guarantee a 10–15% runoff reduction compared to unaltered conditions.

On the other hand, the RHW system guarantees a good outflow reduction, generally up to 15–20% of the unaltered discharge, with low costs for all case studies. This is because of the roof area and slope distribution in the considered cities. Notwithstanding their limited volume, they could be installed on the vast majority of roofs (i.e. sloped) and thus they can largely contribute, at city scale, to runoff reduction; remarkably, their role is predominant with respect to GRs and MBGRs because the latter can be installed on few locations, although they have larger accumulation volumes.

The comparison between the four possible solutions highlights how the RWH system is generally much more efficient (in economic terms) than MBGRs and GRs, with intensive and extensive configuration, and it guarantees a higher reduction of the total city outflow at lower costs. For locations A3 and C1, the maximum flood reduction achievable with MBGRs is higher than with the other solutions, but RWH tanks are less expensive.

GRs and especially MBGRs, however, present many additional benefits for the creation of smart and resilient cities, that need to be considered by policy makers and urban planners: a large-scale installation of these tools can ensure, for example, a significant carbon sequestration and can support the development of the ecosystem, increasing the biodiversity and reducing the urban heat island. A large-scale installation of GRs and MBGRs in the urban environment can, in fact, contribute to the achievement of several Goals of the 2030 Agenda for Sustainable Development (SDGs) adopted by all Member States of the United Nations (e.g. SDG3 Good health and well-being, SDG11 Sustainable cities and communities, SDG13 Climate action, SDG15 Life on land among the others). Moreover, the aesthetic value of the city largely profits from GR or MBGR installations, while RWH tanks could have a negative impact on the urban environment.

5. Conclusions

In this work, the potential impact of blue-green solution installation on flood mitigation was investigated at large urban scale. The installation of green roofs (GRs), with extensive or intensive configurations, or multilayer blue-green roofs (MBGRs), on flat roofs and rainwater harvesting (RWH) tanks for sloped ones was simulated for 9 cities around the world, characterized by different climatological conditions. Several scenarios were investigated to compare the benefits of different combinations of extensive and intensive GRs, MBGRs and/or RWH systems with respect to a non-intervention option. In our study we focused on the highest observed rainfall events, in order to analyse the potential flood reduction and the effect on the lag between rainfall and runoff generation from buildings.

At large scale, GR, MBGR and RWH mitigation performances are strongly related to the roof area and slope distribution that characterizes the city: in most cities the total area of sloped rooftops is larger than flat roof surfaces, while only few cities have a similar extension of flat and sloped roofs. Consequently, in most of the investigated cities, RWH has a larger potential in

discharge reduction, since RWH systems are the most flexible solution for sloped roofs. Moreover, the cost-efficiency analysis developed in this work shows how the RWH installation over the entire city is less expensive and generally more efficient than the GR or MBGR installation to reduce urban floods, in agreement with the preliminary findings presented by CRISTIANO et al. (2021b).

However, if one considers small spatial scale (i.e. the building scale) and extreme events, MBGRs and intensive GR installation ensure higher retention performances and higher delays in the runoff generation. Both in terms of storage capacity and delay between rainfall and runoff generation, MBGRs outperform GRs and RWH systems. These nature-based solutions, moreover, guarantee multiple benefits, such as a strengthening of biodiversity due to an increase in green areas, thermal insulation for the building and added aesthetic value, and they can contribute to the achievement of the SDGs and to the development of smart and resilient cities. For these reasons, the installation of GRs or MBGRs should always be evaluated by policy makers and urban planners.

Finally, it is worth noting that GR and MBGR performance is strongly related to the climatic conditions: results reported in this study showed how the retention capacity is higher if the evapotranspiration and rainfall are in phase (e.g. climatic scenario C defined in Section 2), confirming the conclusions presented in Viola, Hellies, And Deidda (2017). Thus, if two locations with similar rainfall rate (same h_{95}) but different climatic scenario, such as, for example, Airdrie (C1) and Cagliari (D1), are compared, the GR and MBGR retention capacity is higher where rainfall and evapotranspiration are in phase (Airdrie in our example). Similar conclusions can be derived when comparing Waterloo (A2) to Wellington (D3): although they are characterized by the same h_{95}, the GR and MBGRs performance is lower in Wellington, where rainfall and evapotranspiration present asynchronous peaks.

The lack of high resolution freely available data in some regions, such as Asia or Africa has been a limitation for this study. Although all the climatic scenarios are represented, architectural and urbanistic characteristics typical of Asian or African cities, which are not investigated in this study, could have a strong influence on the flood mitigation capacity of blue-green solutions at large urban scale. This aspect needs to be included in future studies, to guarantee a sustainable urban development of these areas, which often have to deal with pluvial floods (Rana et al. 2021; Kazi 2014; Douglas 2017)

In conclusion, the combination of MBGRs for flat surfaces and RWH tanks for sloped ones is the most efficient solution to reduce the flood risk, exploiting all the available roofs. This combination ensures, during extreme rainfall events a minimum discharge reduction of 2% in all locations, reaching 10–16% in Airdrie and Montreal. The potential maximum discharge reduction (20–25%) is achievable with the combination of RWH systems and either intensive GRs or MBGRs. The mitigation performances present high variability, which depends on the antecedent weather conditions, and deteriorate for rainfall events exceeding h_{95} .

Acknowledgement

This work has been partially funded by Fondazione di Sardegna, project: "Green Roofs as smart tool for urban adaptation to climate changes", CUP: F73C22001280007. This work has been partially funded by the ARSINOE project, which has received funding from the European Union's Horizon H2020 innovation action programme under grant agreement 101037424.

Disclosure statement

No potential conflict of interest was reported by the authors.

ORCID

Elena Cristiano http://orcid.org/0000-0002-0725-3014
Stefano Farris http://orcid.org/0000-0002-5039-0575
Roberto Deidda http://orcid.org/0000-0001-5469-0199
Francesco Viola http://orcid.org/0000-0003-1716-192X

List of abbreviations and symbols

Symbol		Description
Abbreviations	*CCDF*	Complementary cumulative distribution function
	DSM	Digital Surface Model
	EHSM	Ecohydrological Streamflow Model
	GHCN	Global Historical Climate Network
	GR	Green roof
	MBGR	Multilayer blue green roof
	RWH	Rainwater Harvesting
	SDG	Sustainable Development Goal
Discharge Estimation	h_{95}	95%-quantile of the non-zero rainfall time series
	Q_0	Discharge in unaltered conditions
	ΔQ_*	Discharge reduction in each scenario
	i	Average rainfall intensity over the area at daily scale
	A	Total urban watershed area
	φ	Runoff coefficient
	$A_{\#}$	Total area for different land use (where # can be green areas, buildings, or roads)
	$\varphi_{\#}$	Runoff coefficient for different land use (where # can be green areas, buildings, or roads)
	$\overline{\Delta Q_*}$	Mean discharge reduction
	$\overline{Q_{095}}$	Mean discharge generation in unaltered conditions
	$\overline{Q_{*95}}$	Mean discharge generation in different scenarios
Green roof parameters	n	Porosity
	Z_r	Soil depth
	S_{fc}	Field capacity
	S_u	Hygroscopic point
	K_c	Vegetational coefficient

References

Adugna, D., Jensen, M. B., Lemma, B., & Gebrie, G. S. 2018. "Assessing the Potential for Rooftop Rainwater Harvesting from Large Public Institutions." *Int J Environ Res Public Health* 15: 2.

Akter, A., and S. Ahmed. 2015. "Potentiality of Rainwater Harvesting for an Urban Community in Bangladesh." *Journal of Hydrology* 528: 84–93. doi:10.1016/j.jhydrol.2015.06.017.

Alidoost, F., and H. Arefi. 2018. "A CNN-Based Approach for Automatic Building Detection and Recognition of Roof Types Using A Single Aerial Image." *PFG - Journal of Photogrammetry, Remote Sensing and Geoinformation Science* 86 (5–6): 235–248. doi:10.1007/s41064-018-0060-5.

Andenæs, E., Kvande, T., Muthanna, T. M., & Lohne, J. 2018. "Performance of Blue-Green Roofs in Cold Climates: A Scoping Review." *Buildings* 8 (4): 55.

doi:10.3390/buildings8040055.
Anon. 2016. "Rise of the City." *Science* 352 (6288): 906–907.
Araujo, M. C., Leão, A. S., de Jesus, T. B., & Cohim, E. 2021. "The Role of Rainwater Harvesting in Urban Stormwater Runoff in the Semiarid Region of Brazil." *Urban Water Journal* 18 (4): 248–256.
Aronica, G., and M. Cannarozzo. 2000. "Studying the Hydrological Response of Urban Catchments Using a semi-distributed Linear non-linear Model." *Journal of Hydrology* 238 (1): 35–43. doi:10.1016/S0022-1694(00)00311-5.
Becciu, G., and A. Paoletti. 2000. "Moments of Runoff Coefficient and Peak Discharge Estimation in Urban Catchments." *Journal of Hydrologic Engineering* 5 (2): 197–205. doi:10.1061/(ASCE)1084-0699(2000)5:2(197).
Beckers, B., J. Berking, and B. Schütt. 2013. "Ancient Water Harvesting Methods in the Drylands of the Mediterranean and Western Asia." *Journal for Ancient Studies* 2: 145–164.
Berardi, U., A. Ghaffarianhoseini, and A. Ghaffarianhoseini. 2014. "State-of-the-art Analysis of the Environmental Benefits of Green Roofs." *Applied Energy* 115: 411–428.
Beumier, C., and M. Idrissa. 2016. "Digital Terrain Models Derived from Digital Surface Model Uniform Regions in Urban Areas." *International Journal of Remote Sensing* 37 (15): 3477–3493.
Bevilacqua, P. 2021. "The Effectiveness of Green Roofs in Reducing Building Energy Consumptions across Different Climates. A Summary of Literature Results." *Renewable and Sustainable Energy Reviews* 151: 111523. doi:10.1016/j.rser.2021.111523.
Bianchini, F., and K. Hewage. 2012. "Probabilistic Social cost-benefit Analysis for Green Roofs: A Lifecycle Approach." *Building and Environment* 58: 152–162. doi:10.1016/j.buildenv.2012.07.005.
Black, Duncan, and Vernon Henderson. 1999. "A Theory of Urban Growth." *Journal of Political Economy* 107 (2): 252–284. doi:10.1086/250060.
Busker, T., H. de Moel, T. Haer, M. Schmeits, B. van den Hurk, K. Myers, D G. Cirkel, *et al*. 2022. "Blue-green Roofs with forecast-based Operation to Reduce the Impact of Weather Extremes". *Journal of Environmental Management* 301: 113750. doi:10.1016/j.jenvman.2021.113750.
Calheiros, C. S. C., and A. I. Stefanakis. 2021. "*Circular Economy and Sustainability*." 1 (1): 395–411.
Alberto Campisano, David Butler, Sarah Ward, Matthew J. Burns, Eran Friedler, Kathy DeBusk, Lloyd N. Fisher-Jeffes, Enedir Ghisi, Ataur Rahman, Hiroaki Furumai, Mooyoung Han 2017. "Urban Rainwater Harvesting Systems: Research, Implementation and Future Perspectives." *Water Res* 115: 195–209.
Chen, Z., B. Gao, and B. Devereux. 2017. "State-of-the-Art: DTM Generation Using Airborne LIDAR Data." *Sensors (Basel, Switzerland)* 17 (1): 150. doi:10.3390/s17010150.
Cipolla, S. S., Maglionico, M., Semprini, G., Villani, V., & Bonoli, A. 2018. "Green Roofs as a Strategy for Urban Heat Island Mitigation in Bologna (Italy)." *Acta Horticulturae* (1215): 295–300. doi:10.17660/ActaHortic.2018.1215.54.
Clapp, R. B., and G. M. Hornberger. 1978. "Empirical Equations for Some Soil Hydraulic Properties." *Water Resources Research* 14 (4): 601–604. doi:10.1029/WR014i004p00601.
Cristiano, E., R. Deidda, and F. VIOLA. 2020. "Ehsmu: A New Ecohydrological Streamflow Model to Estimate Runoff in Urban Areas." *Water Resources Management* 34 (15): 4865–4879. doi:10.1007/s11269-020-02696-0.
Cristiano, E., R. Deidda, and F. Viola. 2021a. "The Role of Green Roofs in Urban Water-Energy-Food-Ecosystem Nexus: A Review." *Science of the Total Environment* 756: 143876.
Cristiano, E., Farris, S., Deidda, R., & Viola, F. 2021b. "Comparison of blue-green Solutions for Urban Flood Mitigation: A multi-city large-scale Analysis." *PLOS ONE* 16 (1): e0246429. doi:10.1371/journal.pone.0246429.
Cristiano, E., ten Veldhuis, M. C., Wright, D. B., Smith, J. A., & van de Giesen, N. 2019. "The Influence of Rainfall and Catchment Critical Scales on Urban Hydrological Response Sensitivity." *Water Resources Research* 55 (4): 3375–3390. doi:10.1029/2018WR024143.
Czemiel Berndtsson, J. 2010. "Green Roof Performance Towards Management of Runoff Water Quantity and Quality: A Review." *Ecological Engineering* 36 (4): 351–360.
Depietri, Y., and T. Mcphearson. 2017. "Integrating the Grey, Green, and Blue in Cities: Nature-Based Solutions for Climate Change Adaptation and Risk Reduction." In *Nature-Based Solutions to Climate Change Adaptation in Urban Areas: Linkages between Science, Policy and Practice*, edited by N. Kabisch, Korn, H., Stadler, J., & Bonn, A. 91–109. Cham: Springer International Publishing.
Douglas, I. 2017. "Flooding in African Cities, Scales of Causes, Teleconnections, Risks, Vulnerability and Impacts." *International Journal of Disaster Risk Reduction* 26: 34–42.
Dwivedi, A., and Buddhiraju K. Mohan. 2018. "Impact of Green Roof on Micro Climate to Reduce Urban Heat Island." *Remote Sensing Applications: Society and Environment* 10: 56–69. doi:10.1016/j.rsase.2018.01.003.
Ellis, E. A., and A. J. Mathews. 2019. "Object-based Delineation of Urban Tree Canopy: Assessing Change in Oklahoma City, 2006–2013." *Computers, Environment and Urban Systems* 73: 85–94. doi:10.1016/j.compenvurbsys.2018.08.006.
Feng, H., and K. N. Hewage. 2018. "Chapter 4.5 - Economic Benefits and Costs of Green Roofs." In *Nature Based Strategies for Urban and Building Sustainability*, edited by G. Pérez and K. PERINI, 307–318, Oxford, UK: Butterworth-Heinemann.
Tim D. Fletcher, William Shuster, William F. Hunt, Richard Ashley, David Butler, Scott Arthur, Sam Trowsdale,Sylvie Barraud, Annette Semadeni-Davies, Jean-Luc Bertrand-Krajewski, Peter Steen Mikkelsen, Gilles Rivard, Mathias Uhl, Danielle Dagenais and Maria Viklander. 2015. "SUDS, LID, BMPs, WSUD and More – The Evolution and Application of Terminology Surrounding Urban Drainage." *Urban Water Journal* 12 (7): 525–542.
Freni, G., and L. Liuzzo. 2019. "Effectiveness of Rainwater Harvesting Systems for Flood Reduction in Residential Urban Areas." *Water* 11 (7): 1389.
Garau, M., Badas, M. G., Ferrari, S., Seoni, A., & Querzoli, G. 2018. "Turbulence and Air Exchange in a Two-Dimensional Urban Street Canyon between Gable Roof Buildings." *Boundary-Layer Meteorology* 167 (1): 123–143.
Gires, A., Abbes, J. B., Paz, I. D. S. R., Tchiguirinskaia, I., & Schertzer, D. 2018. "Multifractal Characterisation of A Simulated Surface Flow: A Case Study with Multi-Hydro in Jouy-en-Josas, France." *Journal of Hydrology* 558: 482–495.
Gomes, R., Galvão, J., Gala, P., Prola, L., & Ribeiro, V. (2021, May) An Overview of Green Roofs in Urban Areas: Impact on Buildings and Food-Energy-Water Nexus. In International Conference on Water Energy Food and Sustainability (pp. 626–635). Springer, Cham.
Gonsalves, S., Starry, O., Szallies, A., & Brenneisen, S. 2022. "The Effect of Urban Green Roof Design on Beetle Biodiversity." *Urban Ecosystems* 25 (1): 205–219.
He, Y., Yu, H., Ozaki, A., & Dong, N. 2020. "Thermal and Energy Performance of Green Roof and Cool Roof: A Comparison Study in Shanghai Area." *Journal of Cleaner Production* 267: 122205.
Hellies, M., R. Deidda, and F. Viola. 2018. "Retention Performances of Green Roofs Worldwide at Different Time Scales." *Land Degradation & Development* 29 (6): 1940–1952.
Huang, C. L., Hsu, N. S., Wei, C. C., & Luo, W. J. 2015. "Optimal Spatial Design of Capacity and Quantity of Rainwater Harvesting Systems for Urban Flood Mitigation." *Water* 7 (9): 5173–5202.
IPCC 2022. Climate Change 2022: Impacts, Adaptation and Vulnerability. "Contribution of Working Group II to the Sixth Assessment Report of the Intergovernmental Panel on Climate Change [H.-O. Pörtner, D.C. Roberts, M. Tignor, E.S. Poloczanska, K. Mintenbeck, A. Alegría, M. Craig, S. Langsdorf, S. Löschke, V. Möller, A. Okem, B. Rama (EdS.)]." *Cambridge University Press. Cambridge University Press, Cambridge, UK and New York, NY, USA*, 3056 pp.
Jamali, B., P. M. Bach, and A. Deletic. 2020. "Rainwater Harvesting for Urban Flood Management – An Integrated Modelling Framework." *Water Research* 171: 115372.
Karteris, M., Theodoridou, I., Mallinis, G., Tsiros, E., & Karteris, A. 2016. "Towards a Green Sustainable Strategy for Mediterranean Cities: Assessing the Benefits of large-scale Green Roofs Implementation in Thessaloniki, Northern Greece, Using Environmental Modelling, GIS and Very High Spatial Resolution Remote Sensing Data." *Renewable and Sustainable Energy Reviews* 58: 510–525.
Kazi, A. 2014. "A Review of the Assessment and Mitigation of Floods in Sindh, Pakistan." *Natural Hazards* 70 (1): 839–864.
Khare, V. R., A. Vajpai, and D. Gupta. 2021. "A Big Picture of Urban Heat Island Mitigation Strategies and Recommendation for India." *Urban Climate* 37: 100845.

Kuichling, E. 1889. "The Relation between the Rainfall and the Discharge of Sewers in Populous Districts." *Transactions of the American Society of Civil Engineers* 20 (1): 1–56.

Laio, F., Porporato, A., Ridolfi, L., & Rodriguez-Iturbe, I. 2001. "Plants in Water Controlled ecosystems_Probabilistic Soil Moisture Dynamics." *Advances in Water Resources* 24: 707–723.

Li, Y., Z. Lin, and H. Shimamura. 2008. "Integrated Method of Building Extraction from Digital Surface Model and Imagery." *The International Archives of the Photogrammetry, Remote Sensing and Spatial Information Sciences* 37: 81–86.

Liu, M., Vecchi, G. A., Smith, J. A., & Knutson, T. R. 2019b. "Causes of Large Projected Increases in Hurricane Precipitation Rates with Global Warming." *Npj Climate and Atmospheric Science* 2 (1): 38.

Liu, W., Feng, Q., Chen, W., & Wei, W. 2020. "Assessing the Runoff Retention of Extensive Green Roofs Using Runoff Coefficients and Curve Numbers and the Impacts of Substrate Moisture." *Hydrology Research* 51 (4): 635–647.

Liu, L., O. Fryd, and S. Zhang. 2019a. "Blue-Green Infrastructure for Sustainable Urban Stormwater Management—Lessons from Six Municipality-Led Pilot Projects in Beijing and Copenhagen." *Water* 11 (10): 2024.

Locatelli, L., Mark, O., Mikkelsen, P. S., Arnbjerg-Nielsen, K., Jensen, M. B., & Binning, P. J. 2014. "Modelling of Green Roof Hydrological Performance for Urban Drainage Applications." *Journal of Hydrology* 519: 3237–3248.

Löwe, R., Urich, C., Domingo, N. S., Mark, O., Deletic, A., & Arnbjerg-Nielsen, K. 2017. "Assessment of Urban Pluvial Flood Risk and Efficiency of Adaptation Options through Simulations – A New Generation of Urban Planning Tools." *Journal of Hydrology* 550: 355–367.

Mahdiyar, A., Tabatabaee, S., Sadeghifam, A. N., Mohandes, S. R., Abdullah, A., & Meynagh, M. M. 2016. "Probabilistic Private cost-benefit Analysis for Green Roof Installation: A Monte Carlo Simulation Approach." *Urban Forestry & Urban Greening* 20: 317–327.

Mainzer, K., Killinger, S., McKenna, R., & Fichtner, W. 2017. "Assessment of Rooftop Photovoltaic Potentials at the Urban Level Using Publicly Available Geodata and Image Recognition Techniques." *Solar Energy* 155: 561–573.

Martin, W. D., and N. B. Kaye. 2020. "A Simple Method for Sizing Modular green–blue Roof Systems for Design Storm Peak Discharge Reduction." *SN Applied Sciences* 2 (11): 1874.

Menne, M. J., Durre, I., Vose, R. S., Gleason, B. E., & Houston, T. G. 2012. "An Overview of the Global Historical Climatology Network-Daily Database." *Journal of Atmospheric and Oceanic Technology* 29 (7): 897–910.

Mentens, J., D. Raes, and M. Hermy. 2006. "Green Roofs as a Tool for Solving the Rainwater Runoff Problem in the Urbanized 21st Century?" *Landscape and Urban Planning* 77 (3): 217–226.

Molaei, O., M. Kouchakzadeh, and F. H. Fashi. 2019. "Evaluation of Rainwater Harvesting Performance for Water Supply in Cities with Cold and semi-arid Climate." *Water Science and Technology: Water Supply* 19 (5): 1322–1329.

G. Myhre, K. Alterskjær, C. W. Stjern, Ø. Hodnebrog, L. Marelle, B. H. Samset, J. Sillmann, N. Schaller, E. Fischer, M. Schulz & A. Stohl. 2019. "Frequency of Extreme Precipitation Increases Extensively with Event Rareness under Global Warming." *Scientific Reports* 9 (1): 16063.

Nachson, U., Silva, C. M., Sousa, V., Ben-Hur, M., Kurtzman, D., Netzer, L., & Livshitz, Y. 2022. "New Modelling Approach to Optimize Rainwater Harvesting System for non-potable Uses and Groundwater Recharge: A Case Study from Israel." *Sustainable Cities and Society* 85: 104097.

Erica Oberndorfer, Jeremy Lundholm, Brad Bass, Reid R. Coffman, Hitesh Doshi, Nigel Dunnett, Stuart Gaffin, Manfred Köhler, Karen K. Y. Liu, Bradley Rowe. 2007. "Green Roofs as Urban Ecosystems: Ecological Structures, Functions, and Services." *BioScience* 57 (10): 823–833.

Susana Ochoa-Rodriguez , Li-Pen Wang, Auguste Gires, Rui Daniel Pina, Ricardo Reinoso-Rondinel, Guendalina Bruni, Abdellah Ichibac, Santiago Gaitan, Elena Cristiano, Johanvan Assel, Stefan Kroll, Damian Murlà-Tuyls, Bruno Tisserand, Daniel Schertzer, Ioulia Tchiguirinskaia, Christian Onof, Patrick Willems, Marie-Claire ten Veldhuis. 2015. "Impact of Spatial and Temporal Resolution of Rainfall Inputs on Urban Hydrodynamic Modelling Outputs: A multi-catchment Investigation." *Journal of Hydrology* 531: 389–407.

Palla, A., Gnecco, I., Lanza, L. G., & La Barbera, P. 2012. "Performance Analysis of Domestic Rainwater Harvesting Systems under Various European Climate Zones." *Resources, Conservation and Recycling* 62: 71–80.

Palla, A., I. Gnecco, and LA Barbera. 2017. "The Impact of Domestic Rainwater Harvesting Systems in Storm Water Runoff Mitigation at the Urban Block Scale." *Journal of Environmental Management* 191: 297–305.

Pelorosso, R., Petroselli, A., Apollonio, C., & Grimaldi, S. "Blue-Green Roofs: Hydrological Evaluation of a Case Study in Viterbo, Central Italy. Ed." *IIn International Conference on Innovation in Urban and Regional Planning* Springer, Cham, 2021. (pp. 3–13).

Pina, R. D., Ochoa-Rodriguez, S., Simões, N. E., Mijic, A., Marques, A. S., & Maksimović, Č. 2016. "Semi- Vs. Fully-Distributed Urban Stormwater Models: Model Set up and Comparison with Two Real Case Studies." *Water* 8 (2): 58.

Rademacher, A. 2019. "Why Cities?" *Science* 364 (6437): 245.

Rajasekhar, M., Gadhiraju, S. R., Kadam, A., & Bhagat, V. 2020. "Identification of Groundwater recharge-based Potential Rainwater Harvesting Sites for Sustainable Development of a Semiarid Region of Southern India Using Geospatial, AHP, and SCS-CN Approach." *Arabian Journal of Geosciences* 13 (1): 24.

Rana, I. A., Bhatti, S. S., Jamshed, A., & Ahmad, S. 2021. "An Approach to Understanding the Intrinsic Complexity of Resilience against Floods: Evidences from Three Urban Communities of Pakistan." *International Journal of Disaster Risk Reduction* 63: 102442.

Rosasco, P., and K. Perini. 2019. "Selection of (Green) Roof Systems: A Sustainability-Based Multi-Criteria Analysis." *Buildings* 9 (5): 134.

Jeetendra Sahani, Prashant Kumara, Sisay Debele, Christos Spyrouc, Michael Loupisd, Leonardo Aragão, Federico Porcù, Mohammad Aminur Rahman Shah, Silvana Di Sabatino. 2019. "Hydro-meteorological Risk Assessment Methods and Management by nature-based Solutions." *Science of the Total Environment* 696: 133936.

Santos, T., J. Tenedório, and J. Gonçalves. 2016. "Quantifying the City's Green Area Potential Gain Using Remote Sensing Data." *Sustainability* 8: 12.

Schultz, I., D. J. Sailor, and O. Starry. 2018. "Effects of Substrate Depth and Precipitation Characteristics on Stormwater Retention by Two Green Roofs in Portland OR." *Journal of Hydrology: Regional Studies* 18: 110–118.

Solcerova, A., van de Ven, F., Wang, M., Rijsdijk, M., & van de Giesen, N. 2017. "Do Green Roofs Cool the Air?" *Building and Environment* 111: 249–255.

Stovin, V., G. Vesuviano, and H. Kasmin. 2012. "The Hydrological Performance of a Green Roof Test Bed under UK Climatic Conditions." *Journal of Hydrology* 414-415: 148–161.

Teston, A., Piccinini Scolaro, T., Kuntz Maykot, J., & Ghisi, E. 2022. "Comprehensive Environmental Assessment of Rainwater Harvesting Systems: A Literature Review." *Water* 14 (17): 2716.

Thornthwaite, C. W. 1948. "An Approach toward a Rational Classification of Climate." *Geographical Review* 38 (1): 55–94.

UN 2018. 2018. "United Nations Final Report on World Urbanization Prospects."

Velasco-Muñoz, J. F., *et al*. 2019. "Rainwater Harvesting for Agricultural Irrigation: An Analysis of Global Research." *Water* 11 (7): 1320.

Vijayaraghavan, K. 2016. "Green Roofs: A Critical Review on the Role of Components, Benefits, Limitations and Trends." *Renewable and Sustainable Energy Reviews* 57: 740–752.

Villarreal, E. L., and L. Bengtsson. 2005. "Response of a Sedum green-roof to Individual Rain Events." *Ecological Engineering* 25 (1): 1–7.

Viola, F., M. Hellies, and R. Deidda. 2017. "Retention Performance of Green Roofs in Representative Climates Worldwide." *Journal of Hydrology* 553: 763–772.

Viola, F., D. Pumo, and L. V. Noto. 2014. "EHSM: A Conceptual Ecohydrological Model for Daily Streamflow Simulation." *Hydrological Processes* 28 (9): 3361–3372.

Weidner, U. 1997. "Digital Surface Models for Building Extraction." In *Basel: Automatic Extraction of Man-Made Objects from Aerial and Space Images (II)* Springer: Science & Business Media, edited by A. Gruen, E. P. Baltsavias, and O. Henricsson, 193–202.

Wen, D., Huang, X., Zhang, A., & Ke, X. 2019. "Monitoring 3D Building Change and Urban Redevelopment Patterns in Inner City Areas of Chinese Megacities Using multi-view Satellite Imagery." *Remote Sensing* 11: 7.

Wooster, E. I. F., Fleck, R., Torpy, F., Ramp, D., & Irga, P. J. 2022. "Urban Green Roofs Promote Metropolitan Biodiversity: A Comparative Case Study." *Building and Environment* 207: 108458.

Wright, J., Lytle, J., Santillo, D., Marcos, L., & Mai, K. V. 2021. "Addressing the Water–Energy–Food Nexus through Enhanced Green Roof Performance." *Sustainability* 13: 4.

Yu, B., Liu, H., Wu, J., Hu, Y., & Zhang, L. 2010. "Automated Derivation of Urban Building Density Information Using Airborne LiDAR Data and object-based Method." *Landscape and Urban Planning* 98 (3): 210–219.

ZHANG, L., L. ZHANG, and B. DU. 2016. "Deep Learning for Remote Sensing Data: A Technical Tutorial on the State of the Art." *IEEE Geoscience and Remote Sensing Magazine* 4 (2): 22–40.

Zhou, D., Liu, Y., Hu, S., Hu, D., Neto, S., & Zhang, Y. 2018. "Green Roof Simulation with a Seasonally Variable Leaf Area Index." *Energy and Buildings* 174: 156–167.

Zhou, L. W., Wang, Q., Li, Y., Liu, M., & Wang, R. Z. 2019. "Assessing the Hydrological Behaviour of large-scale Potential Green Roofs Retrofitting Scenarios in Beijing." *Urban Forestry & Urban Greening* 40: 105–113.